THE CURRENTS OF CASCO BAY
AND THE PREDICTION OF OIL SPILL TRAJECTORIES

by

Charles E. Parker

THE CURRENTS OF CASCO BAY

AND THE PREDICTION OF OIL SPILL TRAJECTORIES

by

Charles E. Parker

Prepared for: State of Maine

State Planning Office
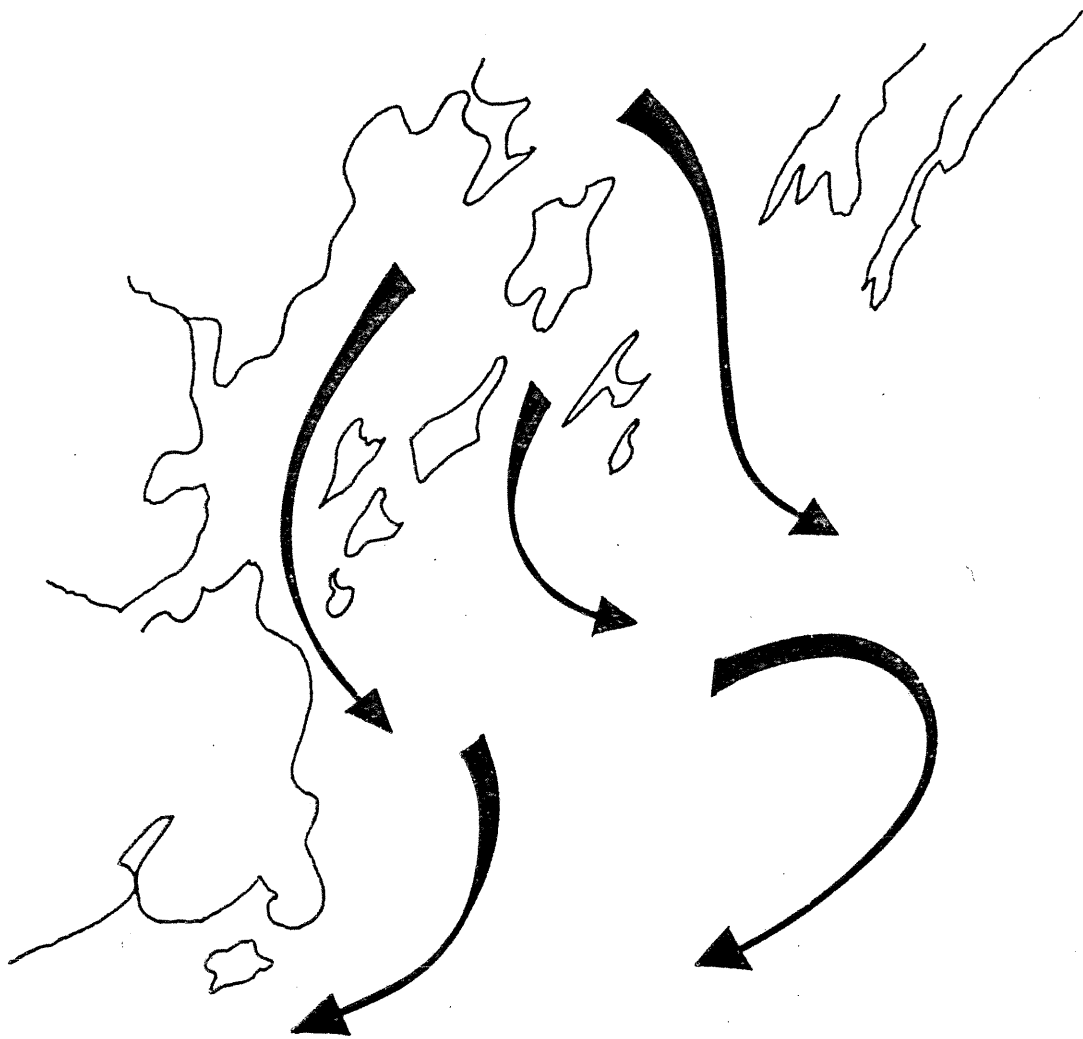
Augusta, Maine 04333

Bigelow Laboratory for Ocean Sciences

West Boothbay Harbor, Maine 04575

Technical Report No. 28   November 1982

PREFACE

This is one of two reports describing the results of an oceano-
graphic survey dealing with the currents and biology and chemistry of
Casco Bay. The aim of this report is to provide pertinent data on the
marine system for the prediction of oil spill movements and contains
information on the tidal and non-tidal currents, water column structure
and bottom topography of the area showing how they interrelate to affect
the deposition of such materials introduced into the system. Additional
discussions on the analysis of wind driven circulation and its effect on
the movements of surface oil are included.

ACKNOWLEDGEMENTS

TABLE OF CONTENTS

INTRODUCTION AND BACKGROUND

The Coastal Energy Impact Program (CEIP) was established in 1976 as
a result of an amendment to the Coastal Zone Management Act. This
amendment provided support to local and state governments to plan for an
alleviate the adverse effects of energy facility development and
attendant activities in the coastal area. This type of development may
have considerable environmental impact on the marine system effecting
such factors as water quality, fishing, the growth of marine plants,
smaller organisms which are important members of the food web, and on
recreation. In order to formulate intelligent and rational plans for
energy development and suitable strategies for consequent activities,
the State recognized the need for detailed information about the marine
environment where many of these activities will take place. With the
exception of a few scattered observations along the coast, this vital
information has not been available in any coherent form. This report is
the result of a two year study by Bigelow Laboratory supported by the
CEIP, on the hydrography and currents found in the Portland Harbor and
Casco Bay region with particular reference to the movement, dispersal
and possible fate of hydrocarbons and other miscible pollutants and
materials which may be introduced into the system. The Casco Bay region
study area is shown in Figures 1 and 2.

We have been fortunate so far. The coast of Maine has yet to be
subjected to a major oil spill or other large scale discharge of
pollutants into its waters. Given the conditions of long periods of
inclement weather, submerged ledges, narrow channels, strong large
amplitude tides, coupled with a steady growth in marine related traffic

and the increased financial pressures to move that traffic through the area at a faster pace, our good fortune may be short-lived.

Currently, over 1,000 ships carrying more than 18 million short tons of cargo (the majority of which is petroleum) enter Portland Harbor each year. In addition to this traffic, another 3.1 million short tons are delivered to Portsmouth with lesser amounts going into ports such as Bath, Searsport, Ellsworth, Bangor and Eastport. Concurrent with these activities, the Bath Iron Works has extensive shipbuilding and repair facilities on the Kennebec River and plans for expansion of those facilities at Portland. This will result in an increase of large ship traffic. Of course, the fishing industry in Maine is one of the most parts of its economy and is, since the establishment of the 200 mile fishing regulation, on the increase. This also is resulting in an increase of fishing-related traffic of larger sized vessels and development of the Portland Fish Pier. It has also become apparent that the area will experience a dramatic increase in the transport and storage of petroleum products in the near future if proposals for doubling the storage facilities in South Portland and storage of petroleum reserves near Westbrook become a reality. In view of these activities, it is apparent that the potential for marine related accidents is there and increasing.

Historically, when a marine disaster occurs and pollutants such as crude oil or refined products are released into the sea, the first concern is where they will go and at what rate. This question is usually directed first to the local oceanographer or marine laboratory who, for the most part, are not too well prepared to give definitive answers due to the lack of hydrographic data for the specific site in

question. The second step is to put together a hastily assembled ad-hoc group of "experts" to assess the situation, suggest an emergency field program to track the spill, study its effect, and then carry out that program, all within a very short time, the usual results being that when sufficient data for counteraction and assessment is finally obtained, it is of limited value and too late. It is anticipated that the research undertaken and reported upon here will be of value not only in the event of an accidental spill but for planning purposes to prevent one.

The analysis to be presented includes estimates on the expected movement and dispersion of released hydrocarbons under varying conditions of surface wind stress, tide and seasonal changes. The analysis is based on data collected during this study which includes direct measurements of current speed and direction, temperature, salinity, density (calculated), and wind speed and direction. Companion to and in support of these data measurements of nitrate, phosphate, silicate, chlorophyll and plankton concentrations have been obtained. A portion of these latter data are reported here for identification of areas of high biological activity which may result from the action of various currents. Further analysis of chemical and biological data collected during the course of the program is to be covered in greater detail in a companion report.

INSTRUMENTATION AND METHODS

A variety of standard oceanographic instruments were used during the field study phase of the program which permitted us to obtain measurements of temperature and salinity with depth, chlorophyll and nutrient concentrations, water transparency, current speed, and

direction for various levels in the water column. Navigation and station control was accomplished using both Loran-C and a precision ranging radar. A recording depth finder was used for bottom surveys and instrument location. A brief description of these instruments and their methods of use follows.

Temperature and salinity observations were accomplished by three methods. The first method employed a Plessey Model 9060 STD which is a self-contained battery operated device that records both temperature and salinity vs. depth on a cylindrical XX'Y graphic plotter. Certain scale modifications to this instrument have enabled us to resolve both temperature and salinity to depth intervals of less than 1 meter. Measurement accuracy of this instrument for temperature is on the order of $0.2^{\circ}C$ and salinity is 0.2 $^{\circ}/oo$. Although the reading of the analog records is done manually, the task has been expedited by using transparent gridded overlays. The second method of obtaining temperature and salinity information was with a Beckman portable Salinometer Model RS5-3. Although this instrument lacks a depth sensor, the simple expediency of marking the 35 meter cable at one meter intervals permitted us to estimate the depth to about two meters in cases where wire angles were 20° or less. The accuracy of the temperature circuit is about $0.2^{\circ}C$ and that of the salinity circuit is about 0.2 $^{\circ}/oo$. Salinity accuracy was improved somewhat by measuring conductivity and temperature and calculating salinity with a special program written for an HP-67 progammable calculator. This method increased the accuracy for salinity to 0.1 $^{\circ}/oo$. The third method for measuring temperature and salinity was with a calibrated bucket thermometer and by collecting discrete salinity samples from both the surface and subsurface (Niskin

bottle). Later these were analyzed with a Guildline 8400 Autosal Salinometer whose accuracy is 0.002 ^{o}/oo. This technique permitted calibration and correction of the first two methods mentioned above. A total of 197 hydrographic stations were taken during 1980 and 1981. The station positions are plotted in Fig. 3.

One hundred ml of seawater was filtered through a Millipore type HA 0.45 μ pore filter for chlorophyll determinations. The filters were frozen with dry-ice and returned to the laboratory where processing was done using the method of Yentsch and Menzel (1963). These data were used for producing surface chlorophyll maps.

Samples for nutrient analysis were filtered through a Whatman GFC filter (after rinsing with sample water) directly into 128 ml wide mouth Nalgene bottles. Eighty ml of filtrate was frozen to be analyzed for dissolved organic nitrogen, nitrate and nitrite, phosphate and silicate. After thawing in the laboratory, the samples were analyzed using a Technicon autoanalyzer system (Garside *et al.*, 1976). Precision was $\pm$ 0.10 μg-at ℓ^{-1} or better for all measurements.

Water transparency was measured with a Secchi Disc suspended from a line marked off at one meter intervals.

Currents were measured using three basic methods. The first two, surface and subsurface current drogues (Fig. 4) were tracked with the ship and their positions determined periodically with Loran-C and precision ranging radar. Positional errors fall within the range of $\pm$ 100 meters. To facilitate navigation, special small scale Loran-C charts were constructed for the entire area using calibration points supplied by the U.S. Coast Guard, Science Application Corp., Newport, RI plus those taken during the initial phases of the study. In addition to

these charts, a special program was written for the HP-67 calculator
which converted the Loran-C readings to latitude and longitude and
calculated speed and direction from the previous readings in the series.
One to six drogues were followed at a time for periods of up to 12
hours. All drogue measurements were restricted to daylight hours. A
total of 887 hours of current measurements were realized during the
survey.

The third method of measuring currents was with self-recording
current meters anchored to the bottom. These meters (Endeco Type 105
film recording) are of the ducted impeller design and attain resolutions
of 2.6 cm s^{-1} in speed and resolve direction to $\pm 1°$. The scheme of
implacement and retrieval (Fig. 5) was dictated by two factors. One was
the reduction of costs associated with expensive release systems and the
second, the need to place the equipment in such a fashion so as to
prevent vandalism or interference through accidental entanglement of the
mooring lines. The mooring design used throughout the survey was
successful and all current meter stations, a total of ten, were
retrieved. Relocation of the moorings were done with Loran-C and depth
finder which was able to detect and display the position of the
underwater floats. Retrieval was accomplished by lowering a pair of
grapple hooks on a 1/2" line to snag the 400' longitudinal ground lines
suspended above the bottom by aluminum floats. All current meters were
positioned on the suspension line 3.1 meters from the bottom. All film
recordings of the current speed and direction were processed by Endeco
and yielded a total of 2,369 measurement hours, at 15 minute intervals,
in both computer typed format and as progressive vector diagrams.

Another source of current meter data has been made available which has been utilized for the preparation of this report. These data resulted from a survey done by the National Oceanic and Atmospheric Administration (NOAA) during the late summer and early fall of the year preceding the start of our field program (1979). A total of 42 current meters (Grundy/Plessey self recording magnetic tape, 10 minute recording interval) were implaced at 21 separate locations. The majority of these locations were within the bays and channels and complemented our CEIP channel and offshore mooring sites nicely. Both sets of measurements were taken at the same time of the year. We acquired the NOAA records in analog strip chart format and after making the necessary corrections, were read by hand with the help of the HP-67 calculator. Locations for all current meter stations for both NOAA and CEIP surveys are presented in Fig. 6.

A data collection summary for the Coastal Energy Impact Program is given in Table 1.

STUDY AREA DESCRIPTION

The Casco Bay Region (Fig. 2) has, for the purpose of this study, been divided into five oceanographic areas as shown in Fig. 7. These areas or environmental provinces are characterized by different oceanographic, meteorological, topographical features which would, in the event of an accident, be expected to present different patterns for the movement, dispersion and retention of pollutant materials.

1. Portland Harbor: running inside of the major islands from about Fish Point to Cousins Island. This area has the greatest length of

Table 1

Coastal Energy Impact Program Oceanographic Observations

Date	Vessel	Hydrographic Station	Chlorophyll Station	Transparency Station	Nutrients Station	Current Drogues (hours)	Current Meters[1] (hours)	Weather Observations[2]
2/8/80 to 2/9/80	Capricorn and Explorer	123	54	0	31	560	1968	50
1/2/81 to 3/3/81	Challenge	22	0	21	22	73	73	17
8/4/81 to 4/5/81	Capricorn	37	39	73	0	142	306	36
7/8/81 to 1/8/81	Capricorn	15	0	14	0	112	95	18
TOTALS:		197	93	108	53	887	2369	121

Does not include ≈ 10,000 hours of NOAA current meters observations for 1979 used in this analysis.

Weather observations have been supplemented from National Weather Service Observatory publications of Local Climatological Data for the Portland Jetport.

populated shoreline on its northwestern side and is protected from open sea conditions. There are five inlets to the bay area, two of which carry the majority of ship traffic into the harbor as well as the bulk of the tidal flow. The two main channels are through Hussey Sound, between Peaks and Long Island, and the north end of the Portland Channel which includes Diamond Roads. This area has the largest expanse of shallow bottom in the region thus it is expected that there will be a more wind-responsive surface circulation set up here under certain conditions compared to other more protected areas. This area is also characterized by very shallow mud flats and inputs of fresh water drainage from the Presumpscot and Fore Rivers. Included is, of course, the main part of Portland and South Portland Harbors. Temporary anchorage for transient vessels is provided near Great Diamond Island as well as in the State-maintained oil transfer area located in the center of the area northwest of Long Island.

2. Northeast Inner Bay: running northeast from Cousins Island for about 9.3 km. Approximately half of this area is covered by waters of less than 3 meters depth. There are three fresh water drainages in this part of the bay; the Royal, Cousins and Harraseeket Rivers. The major communication with the open sea is through Broad Sound which leads south-southeast from the area. Generally speaking, all of the islands in the bay line up in a northeast to southwest direction and their presence dictates the direction of the flow found there. The broadest extent of mud flats for the Casco Bay Region are located along the northwestern shore.

3. Channels and Islands: running northeast from Portland Head and approximately 18.5 km to Harpswell Neck and includes most of the larger

islands and channels in the region. These channels, Portland Harbor Channel, Whitehead Passage, Hussey Sound, Luckse Sound, Chandler Cove and Broad Sound form the major conduits for the exchange of oceanic and bay waters. Three of these passages have depths between 20 and 35 meters and are known for their swift tidal currents. The bottom in these areas is, for the most part, rocky or rock/mud in nature and shoals rapidly near the islands. On the southeast sides of the islands, surface wave action and water turbulence may be quite severe during times of strong southeast winds. This is not surprising considering the long fetch in this direction.

4. _Casco Bay Basin_: bounded on the southwest by Cape Elizabeth and the channel between the Cape and West Cod Ledge and for the purposes of this study, on the northeast by a line running south along 70° W longitude. The area is semi-enclosed at depths greater than about 20 meters due to the presence of the West Cod Ledge which lays northeast-southwest about 9.3 km offshore of channels and islands. The bottom is mostly rocky and rough with tortuous leads and gullies below 30 meters. West Cod Ledge is the most prominent feature of the area and rises to less than 10 meters of the surface in some places. This 15 km long ledge plays an important part in controlling the general circulation of the entire area as we shall see later. Due to the irregular nature of the bottom current speeds are low and their directions are controlled by the trend of the topography. There is one major communication for the flow of deep bottom water from further offshore northwestwards towards the major island channels. This is found 6 km to the north-northeast between the northeastern tip of West Cod Ledge and Halfway Rock,.

5. <u>Maine Coastal Shelf</u>: designated here as that area found seaward
of West Cod Ledge. This portion of the study area is fairly typical of
much of the southwest Maine mid-shelf region. Surface tidal currents
tend to become more elliptical in direction with speeds slower than
those found nearer shore. Also bottom currents are slower due to the
absence of constricting channels and ledges. Some of the more important
fishing grounds are located here, such as those near the Hue and Cry and
East Cod Ledges.

BOTTOM TOPOGRAPHY

A set of four bottom topography charts have been prepared (Figs.
8-11) which show the aerial extent of waters below the designated depth
for each chart. These charts have been prepared to demonstrate, in a
slightly different manner from usual bottom contour charts, the very
rugged nature of the bottom and serve to highlight the presence of many
narrow constricting channels, isolated edges and shoals. These features
tend to control the flow of water at those depths and consequently the
movement of materials within the water column. I direct the reader's
attention especially to the chart depicting the depth of water found
below 30 meters (Fig. 11). The first obvious feature seen is the
delineation of only one narrow channel on the southeastern edge of the
blackened area which leads into the complex inner portions of the Casco
Bay region. This channel is the only passageway permitting inflow of
deeper offshore waters into the bottom system and conversely the
flushing of the same out of it. The second noteworthy aspect of the
deep topography is the presence of many narrow blind channels,
cul-de-sacs and isolated basins. It must be pointed out at this time

that these types of bottom features can be potential traps and holding areas for whatever materials settle into them. The currents found in and around these depths tend to be very slow. Consequently, the resulting low flushing rates and long residence times of waters found within them become important especially when considering the fates of heavier pollutants. The two other charts presented show, to a lesser extent, essentially the same situation of relief at depths of 10 and 20 meters but there is a greater potential of communication of waters at these levels than those found deeper.

A qualification to statements should be given at this point regarding the exchange and transport of waters in and around these bottom features. Under certain conditions of equal vertical density, tidal forcing and wind stress can set in motion stronger deep currents which will move water from one level to another because of local topographically induced turbulence. These conditions are most likely to occur during the winter when the water column cools from the top down finally reaching temperature values near or colder than those near the bottom and during periods when strong winds may be present.

THE TIDES

The tides of Casco Bay dominate the circulation and continuously affect the distribution of properties found within it. Tides are classified according to the nature of the diurnal or semi-diurnal constituents present. The tidal signature in Casco Bay is identified as a mixed-mainly semi-diurnal flow meaning that successive high or low tides do not have the same amplitude. A sample of the tidal heights for Portland Harbor for September and October 1979 are given in Fig. 12.

This time period includes part of the survey dates for the NOAA current meter measurements. As seen in this diagram, there is a marked difference in amplitude from one part of the month to the next which range from maximums at high tide of 8 to 11 feet to a change in minimum low tide levels of +1.4 to -1.9 feet. The two pair of curves show the cycle of elevation change for alternate high and low tide. These vary by approximately one foot during the time when the moon is in quadriture, for example on about September 16 and 30, to almost amplitude equality at the time of full moon during the first week of September and October. It is sufficient to mention at this point that tidal current speeds at the time of maximum flood vary from about 25 cm/sec (½ knot) offshore to over 90 cm/sec in the more restricted channels. These flows will be discussed in greater detail a little later in this report.

THE PHYSICAL ENVIRONMENT

The following discussion includes the description of the temperature fields observed at various depth, the distribution of density, vertical stability and chlorophyll as they pertain to certain features found regarding the transport of Casco Bay waters. For the sake of clarity, the charts depicting these parameters show the conditions for ebb and for flood tide periods. This division enables us to better demonstrate what changes occur between one tide and the next and how these changes relate to the circulatory system as a whole. It must be kept in mind that any charts presenting data of this sort can never give a true picture of any measured quantity since it is impossible to make simultaneous observations in space and time. The

data shown here were gathered over a period of more than two weeks.
These data were then organized chronologically according to published
times of high and low water at Portland Harbor.

Surface, 5 meters, 10 meters and 15 meters ebb and flood stage
temperature charts for August and September 1980 are given in Figs. 13
to 20. It can readily be seen that there are large differences in the
distribution of temperature which take place during 6 hours and there is
considerable variability at both large and small space scales. For
demonstration purposes, shading has been added to delineate waters
colder than 16.0°C on the surface, colder than 15.0°C at 5 meters,
colder than 13.5°C at 10 meters, and colder than 12.5°C at 15 meters.
This device has been employed for the purpose of highlighting one of the
most important dynamic features of the region, that of persistent
upwelling of water from lower levels. It can be seen that during flood
tide there is a movement towards the shore and channels of deep cold
water up to progressively shallower depths which finally manifests
itself at the surface not only as a large cool pool just outside of
Jewell Island but also well up into the heads of the major channels and
southern parts of the inside bays. The source of this cold water as
seen in Fig. 20 (for 15 meters) is apparently from two bottom areas, one
located southwest of Cape Elizabeth and the other to the east of Halfway
Rock. This flow is even more clearly evidenced in Fig. 19 (for 10
meters) which shows the flow from the east as a large tongue which
reaches the area of Jewell Island cool pool. This flow is probably
augmented from the southwest.

On the ebb tide there is a marked change in the pattern of cold
water found at all depths. At the surface it has receded to some extent

out from the inner bays and upper channels to form a continuous band
along the outer portions of the channels and along the islands. The
cool pool which was centered south of Jewell Island and had extended out
to West Cod Ledge on the incoming tide is not present. A better
indication for the direction of flow during ebb tide can be obtained
from the subsurface temperature charts. At 5 meters (Fig. 14) there is
a retreat of cool water to the southeast from the area between Jewell
Island and the entrance to Broad Sound. At the deeper levels, 10 and 15
meters (Figs. 15 and 16), there is also a recession of cold water to the
east and southeast for a distance of approximately four miles. From the
persistence of cool surface water and the progression of subsurface
tidal events offshore, a general picture of the extent and nature of the
upwelling system begins to emerge.

Further evidence for the presence of an active upwelling system
comes from the study of the water density (a function of both tempera-
ture and salinity) found at one level relative to its surroundings and
analysis of the vertical stability of the water column. Stability is
computed from the differences of density with depth and gives an
indication in certain areas of how materials may move more easily from
one depth to another. Upwelling systems are characterized by values of
low stability which permit vertical transport while horizontal current
regimes are associated with regions of high vertical stability. High
localized surface densities are also good indicators of upwelling.

Figures 21 and 22 showing the distribution of ebb tide surface
density and 0 to 15 meter vertical stability aptly demonstrate that the
waters nearshore and between the islands are directly influenced by the
upwelling of deeper waters. The areas of higher than average density

and low vertical stability have been shaded to highlight those critical areas where upwelling is taking place. These areas coincide with the same areas during the same stage of the tide as those occupied by cooler than average water.

This upwelling is not only responsible for bringing colder more saline water to the surface but also transports from subsurface areas offshore nutrients and biological materials up to the surface layer. Direct evidence for this may be found in Fig. 23 which shows the quantities of chlorophyll a observed during the period of ebb tide. This biological material is found in marine plants called phytoplankton which are primary energy sources for microscopic animals (zooplankton), fish larvae and other organisms living further up the food chain. When upwelling conditions such as those found in Casco Bay are present, the enhanced stirring and turbulence of the water column (due to low vertical stability) brings up nutrients and biological materials to the sunlit surface layer resulting in an increased growth of chlorophyll producing plants. High chlorophyll values (shaded) in Fig. 23 all correspond to the areas previously described as being active upwelling zones. Since the intention of this report is to discuss the movements of pollutants in the Casco Bay area, it is important to point out at this time that neutrally buoyant foreign substances which find their way in to the water column will behave in the same way as those found naturally in the system. These foreign substances will also be carried up to the surface and may affect the growth of both phytoplankton and zooplankton, the primary producers in the food chain.

THE CURRENTS OF CASCO BAY

The primary purpose of this research is to provide information

regarding the nature of the currents in the region in sufficient detail

for the prediction of the movements of hydrocarbons (and any other

pollutant materials) inadvertently introduced into this environment.

Keeping in mind our discussions regarding other physical parameters and

how their distribution gives evidence for dynamic processes operating

within the area, such as the evidence showing the advance and retreat of

cold water with the tide, maintenance of an active upwelling system and

other associated physical and biological changes, we shall now present

the results of the current surveys.

As mentioned earlier in the Methods section, current measurements

were made using a variety of devices. Surface and subsurface current

drogues were our primary tools for obtaining Lagrangian flow measure-

ments; i.e. following the path a water parcel travels. This type of

measurement differs from an Eulerian one such as obtained from a current

meter that senses the flow past a particular point in space. Eulerian

measurements are useful in obtaining current flow time series for

different depths and in the calculation of current shears. Lagrangian

measurements are well suited for the problem at hand since they yield,

if done in the proper manner, a fairly accurate representation of what

the actual trajectory of the flow may be from point to point over any

given period of time. This has been accomplished by putting into play a

number of drogues in a variety of patterns. Since tides are the

dominant oceanic force in this system drogue sets were repeated in

certain areas so that all phases of the tidal cycle currents were

observed. The usual procedure was to set two to four surface drogues in

an area of about four square miles. These were accompanied by one or

two subsurface drogues and all were followed during the day with the

boat and their positions were determined as frequently as possible with

Loran-C or radar. Concurrent with the tracking, measurements of

temperature and salinity with depth were made to determine whether or

not the drogues had stayed with the particular parcel of water it was

originally placed in.

For the purpose of data analysis and presentation all current

measurements have been divided into two hour tidal segments. Two sets

of six charts, each showing the surface and bottom currents for

August/September 1979 and 1980, are given in Figs. 24 to 35. The arrows

show the direction of the current at the place it was measured and the

numbers associated with them give the average speed in cm/sec for the

two hour period. One knot equals 51.44 cm/sec. The dashed lines have

been added for the purpose of providing continuity to the diagrams and

are to be viewed only as an interpretation of the flow pattern between

those actually observed.

SURFACE CURRENTS

One of the outstanding features in all of the current diagrams is

the persistent presence of a surface gyre or circulatory flow located in

the vicinity of West Cod Ledge. This clockwise flow is evidenced during

all stages of the tide varying only in its strength which ranges between

9 and 16 cm/sec on the flooding tide to between 17 and 30 cm/sec on the

ebbing. The presence of the gyre is also indicated in Figure 23 by the

area of low chlorophyll values centered at about $43^{\circ}36'$ and $70^{\circ}05'$. On

the eastern side of the gyre, the flow is south out around the ledge

with no apparent reversal during flood tide. On the western side near Cape Elizabeth there is a reversal in direction to the north on flood tide which shows speeds of about 25 cm/sec. On the ebb tide, these speeds are increased to about 38 cm/sec to the southwest around the Cape. This increase is probably the result of the addition of the westward flowing non-tidal coastal current south of West Cod Ledge to that of the tidally induced flow. It would appear that the non-tidal coastal current in this area is about 10 to 12 cm/sec.

Northwest of the gyre and south of Peaks Island there appears evidence for the formation of a strong divergent flows on the flood and ebb tides where the currents split to enter and leave Portland Harbor Channel, Hussey and Luckse Sounds. The speeds associated with this divergence are on the order of 22 to 28 cm/sec. Cool temperatures and low vertical stabilities shown previously, closely correspond to the location of the divergent area and together give firm evidence for upwelling of bottom waters.

There are a few features of the flow in the major channels which should a be noted. First, during the initial 2 hour stage of the flood tide (Fig. 24), there appears a moderate southerly flow out of Broad Sound and out of Luckse Sound to the southwest, which is contrary to what might be expected especially when contrasted with the strong flows northward into Portland Harbor channel and Hussey Sound at this time. These reverse currents are probably the result of residual draining of waters from the large expanse of shallow upper bays and flats north and east of Broad Sound. Flows into Broad Sound during the latter four hour period of flood tide (Figs. 25 and 26) were the highest measured during the survey (greater than 90 cm/sec) and the resulting extra transport of

water into the system compensates for the shortened period. Current meter records for Broad Sound show that ebb tide flow occurs for 62% of the time and flood tide takes about 35% with about 3% of the flow being weak and variable in direction.

Secondly, an inspection of the chart for the first two hours of ebbing tide (Fig. 27), the currents of Luckse Sound again show unexpected differences in their direction of flow. There is a 25 cm/sec current to the northeast towards Broad Sound instead of in the opposite direction. This may be the result of a venturi effect of the strong southerly currents in Broad Sound and nearby smaller channels which tend to draw water into a portion of Luckse Sound. This northeasterly flow appears to be augmented by the swift (40 cm/sec) flow out of Chandler Cove which turns in this direction around Hope Island.

Table 2 summarizing the surface current flows for various locations is presented for reference of flow conditions for two hour segments of the tidal cycle and for comparison of one area to another. The notations "N" for in or northward flow and "S" for out or southward flow included with the speeds (cm/sec) have been added to clarify the flow direction which, as discussed previously, do not always coincide with the expected ebb and flood conditions.

CURRENTS AT MID-DEPTH

The mid-depth observations of currents indicate that, given a few rules of thumb, estimations of the state of the subsurface flow during any given two periods of the tide are possible and for this reason, it has been decided not to present another series of six mid-depth current charts. Observations show that for depths between 5 and 15 meters the

Table 2

SURFACE CURRENT SUMMARY

2 Hour Average Speed Ranges (cm/sec)

Direction: N, North; S, South

Location	FLOOD			EBB		
	Lo-L2	L2-L4	L4-Ho	Ho-H2	H2-H4	H4-Lo
Cape Elizabeth	15-25N	11-14N	8-9N	9-13S	12-38S	10-30S
Portland Hbr. Chan.	28-39N	55-75N	30-58N	29-30S	31-44S	12-14S
Hussey Sound	22-29N	43-58N	20-51N	13-54S	40-43S	17-28S
Luckse Sound	9-24S	10-30N	10-33N	18-30N	12-29S	10-12S
Broad Sound	7-10S	25-91N	18-51N	5-14S	20-32S	17-22S
House I.	30N	18N	8S	18S	20S	15N
Chandler Cover	37N	29N	17N	40N	31N	17N
Cousins I.	3S	20S	32S	25S	10S	4N

currents within the bays and channels are highly coherent in direction
with the surface current. Changes in direction from that of the surface
flow will be dictated by the trend of the local bottom topography at the
depth of interest. Current speeds are uniformly slower, being reduced
by approximately 30 to 40% of those found at the surface. Tidal
reversals correspond closely with those already shown for the surface.

Offshore in the more open areas, the upper mid-depth (< 15 m)
current speeds are reduced by approximately the same amount as those in
the shallower areas. Deeper than 15 meters, speeds decrease rapidly
approaching those at the bottom. The same holds true for current
direction. Those found above 15 meters are similar to the surface
direction and those below tend to align themselves with the bottom flow
which will be discussed next.

BOTTOM CURRENTS

The bottom measurements as described in this section have been
obtained from two sources as stated earlier. The bottom current data
shown in Figs. 30 to 35 are a combination of both data sets for the
months of late August and early September only. The two series of
observations were in close agreement in speed and direction for those
areas where one set overlapped another even though they were taken one
year apart.

The set of six figures showing the bottom currents have been, as
those for the surface current, divided into two tidal periods and the
arrows showing the direction have been placed at the point of
measurement. The arrows that appear as reversed curves represent flows
that changed direction more than 120 degrees during the indicated two

hour period. Speeds are, as before, noted alongside of their respective directional arrows.

As might be expected the direction of flow near the bottom is highly influenced by the nature of the bottom topography. For example, the clockwise surface flow seen over West Cod Ledge has been modified at depth to either a northerly or southerly going current during the time of maximum flood or ebb except during the four hour period centered on the time of high slack water when a fairly strong flow is present from the east. This westerly flow is responsible for the advance of cold bottom water from the east and appears to be the major driving force for the upwelling described earlier.

Further inshore high bottom current speeds are found in the channel of Hussey Sound where they average well over 40 cm/sec during the last two hours of flood tide and first four hours of the ebb tide. These bottom currents were the highest measured in the area. Maximum bottom currents in the Portland Harbor channel are a little slower (approximately 35 cm/sec) and occur at about the same period of the tide as those in Hussey Sound. Broad Sound, on the other hand, shows tidal flows at the bottom which are out of phase (at the commencement of the flood and ebb periods) with the other channels. Although the speeds are less than in the other two major channels (approximately 22-25 cm/sec) the increased width and breadth of this channel results in a comparable water transport.

The current meter set in the Cousins Island channel shows a southwesterly flow that reaches speeds of 18 cm/sec during the first two hours of ebb tide which contrasts sharply with that of about 4 cm/sec which flows only during the starting hours of the commencement of the

flood tide. These observations are in agreement with the general idea that the timing of the flow reversals in the upper reaches of Broad Sound and its outlets are a result of delayed residual flows from these expansive areas.

CIRCULATION SUMMARY

As we have seen the currents of the Casco Bay region are highly complex in detail while at the same time there is a regular progression of events that lend themselves to a basic understanding of how the system works. The major components of the current system are as follows.

1. The Broad Sound area is for the most part separate from the rest of the bay system except for the shallow channel north of Cousins Island and the narrow channel between Cousins and Great Chebeague Islands. These channels serve mostly to drain some of the water from the upper portions of Broad Sound from the northeast. The total transports are low due to the small cross sections of these channels. The major import and export of water from Broad Sound is through the southern entrance augmented by flows through Luckse Sound. There are tidal phase delays for both the surface and bottom currents.

2. The currents in Hussey and Portland Harbor Channels are in phase with the published tide times. This applies to both surface and bottom currents. The flood tide flow through these channels is supplemented by that flowing between Long Island and Great Chebeague in Chandler Cove.

3. An active upwelling zone is present south of Jewell Island. This upwelling is the result of the divergence of the flood tide surface flow as it enters Portland Harbor Channel, Hussey and Luckse Sounds.

Upwelling is also present at the heads of the major Channels. The forcing of bottom water into increasingly shallower depths during the flood tide is responsible for upwelling in these areas.

4. A clockwise recirculation gyre is maintained near West Cod Ledge throughout most of the tidal cycle. This circulation is a result of both the interference of the shallow ledge to the north-south tidal flow and the diverting of the southwesterly flowing non-tidal coastal current to the north and south of the ledge.

5. Offshore bottom currents are controlled primarily by the bottom topography. The only entrance into the Casco Bay basin for waters below 30 meters is through a narrow passage found between West Cod Ledge and Halfway Rock. Because of the restrictions imposed by the bottom topography it appears that the major flows in and out of the basin must take place at depths shallower than 25 meters.

6. The rapid swing of the ebb tide current between Cape Elizabeth and West Cod Ledge is due to the additive effect of the longshore non-tidal coastal current to that of the tidal flow. This current is estimated at about 10 to 12 cm/sec. The transport of bottom water to the north past Cape Elizabeth occurs only during the first four hours of the flood tide and appears to be small in volume.

THE EFFECT OF WIND ON THE CURRENT

Although the action of the tides constitute the most dominant force for the movement of water in this system the wind also plays an important part in determining the circulation and it must be considered when attempting to estimate the transport of water in shallow systems. It is not intended to give a detailed technical discussion of the

dynamics of wind driven currents for this can be found in most oceanography texts which devote long chapters to the subject but instead, since this report is intended to be a working document for estimating currents, I will give just a few simplified rules for wind drift. There are more elegant methods available but for all practical purposes the following methods give a good approximation of the shallow wind driven current. These rules are sufficient for calculations of flow for the first 15 meters of depth. The deeper currents are more controlled by the bottom topography then they are by the wind.

The following formulas were used to remove the wind current component from the observed measurement of current in order to resolve the true tidal current shown on the charts. Wind speed and direction data were obtained from both records kept at the Portland International Jetport and from direct on-site observations taken during the course of the surveys. From these records the resultant wind was calculated for each 24 hour period prior to each current observation then applied in the correction formulas.

To estimate current speed as a function of wind speed the results of Thorade (1914) have been employed.

For winds of less than 6 meters/sec. (approx. 12 knot) the surface current $Vc = \dfrac{\sqrt{2.59\ W}}{\sqrt{\sin \theta}}$

where: W is the average wind speed in meters/sec,

θ is the latitude of the observation,

Vc is the surface current in cm/sec

For winds greater than 6 meters/sec

$$Vc = \frac{1.26 \ W}{\sqrt{\sin \theta}}$$

To estimate the effect of the wind on the direction of the current
(previous research has shown that the current is deflected to the right
of the wind in the northern hemisphere due to the rotation of the earth)
we have used the results of Witting (1909) which give:

Wd = $(34-7.5 \ \sqrt{W}$) + Wind direction (towards)

where, Wd is the direction of the wind current and

W is the average wind speed in meters/sec.

The graph given in Figure 36 summarizes the above formulas for both
current speed (in linear form) and direction as a function of the wind
(at 43° 38' N) and may be used as a quick reference for estimation of
its effect on the surface currents in Casco Bay. The solid line on the
graph is for current speed (cm/sec) vs wind speed and the dashed line is
for the deflection of the current (degrees) to the right of the wind vs
wind speed (m/sec). For example, if the wind is blowing from the west
(towards 090°) at 8 m/sec the surface current will be approximately 12
cm/sec and the direction will be about 13° to the right of the wind
direction or about 103°. The resultant wind current vector must then be
combined with the non-wind driven current to determine the resultant
true current.

PREDICTION OF CURRENT TRAJECTORIES

Consistent with the original intent of this research it is
important that the data presented serves a practical purpose and that
methods for its application be available. It is evident from the
preceding discussions on the nature of the currents and how they are

effected by the bottom topography, islands and channels and the timing

of the tide that it would be impossible to anticipate all of the cases

where an oil spill could occur and to consider all conditions of tide

and wind at the time of the accident. We can though, with a few

straightforward calculations, together with timely observations of wind

speed and direction, construct adequate first order approximation

trajectories for any given situation that might arise.

It must be kept in mind that the current speed and direction data

given on the charts are average values for two hour segments of the

tidal cycle and as such do not give maximum and minimum speeds or show

small scale streamline curvatures present during any given time period.

Table 3 converts the speed (cm/sec) given on the current charts to

nautical miles displacement for a two hour tidal period.

The following example demonstrates how the current charts, wind

current correction graphs and the speed conversion table may be used to

obtain reasonable estimates of the flow path and the distance a

particular parcel may travel. We will use a starting point at 43° 38'

and 70° 09' or approximately 1 mile east of Peaks Island at low tide

with the resultant wind blowing from the east at 4 m/sec.

The procedure is as follows:

1. Locate on the LO-L2 surface current chart (Fig. 24) the current

vector nearest to 43° 38' and 70° 09' which is 29 cm/sec and, from

measurement with a protractor, has a direction of 215°.

2. From the wind correction graph we find that for a wind speed of

4 m/sec the magnitude of the wind driven current will be about 6.3

cm/sec and it will be deflected about 19° to the right of the wind

direction (towards) or 289°.

Table 3

DISTANCE CONVERSION FOR CENTIMETERS/SECOND (cm/sec) TO NAUTICAL MILES (NM)

Per 2 Hour Tidal Segment

NM = cm/sec (.0389)

cm/sec	0	1	2	3	4	5	6	7	8	9
0	0	.04	.08	.12	.16	.19	.23	.27	.31	.35
.10	.39	.43	.47	.51	.54	.58	.62	.66	.70	.74
20	.78	.82	.86	.89	.93	.97	1.01	1.05	1.09	1.13
30	1.17	1.21	1.24	1.28	1.32	1.36	1.40	1.44	1.48	1.52
40	1.56	1.59	1.63	1.67	1.71	1.75	1.79	1.83	1.87	1.90
50	1.94	1.98	2.02	2.06	2.10	2.14	2.18	2.22	2.26	2.29
60	2.33	2.37	2.41	2.45	2.49	2.53	2.57	2.60	2.64	2.68
70	2.72	2.76	2.80	2.84	2.88	2.92	2.95	2.99	3.03	3.07
80	3.11	3.15	3.19	3.23	3.27	3.33	3.34	3.38	3.42	3.46
90	3.50	3.54	3.58	3.62	3.65	3.69	3.73	3.77	3.81	3.85

3. Construct vector triangle with sides ABC; side A = 6.3, B = 29 and angle c = 180° - (289° - 215°) = 106°.

true curr.
31.22/226.15°

< a=11.15°

obs. curr.
29/215°

wind   270°/4 m/sec

< c=106°
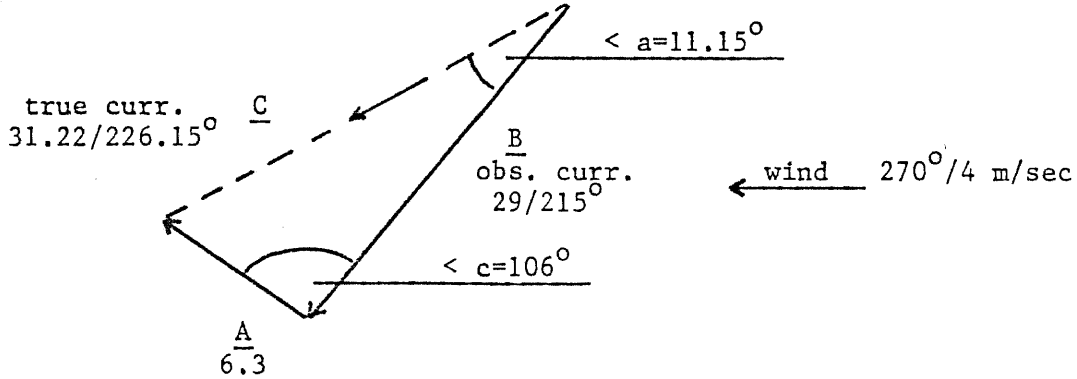
$$\text{Tan a} = \frac{\text{A sin c}}{\text{B} - (\text{A cos c})} = \frac{6.3 \sin 106^{\circ}}{29 - (6.3 \cos 106^{\circ})} = 11.15^{\circ}$$

Therefore the true current direction = 11.15° + 215° = 226.15°.

$$\text{Side C} = \text{A}\frac{\sin c}{\sin a} = 6.3(4.97) = \underline{31.32} \text{ cm/sec which is the true}$$

speed.

4. From Table 3 we find that the two hour tidal period speed of 31.32 cm/sec would equal about 1.22 NM displacement.

If we now plot this vector on a chart we see that at the beginning of two hour tidal period L2-L4 the next trajectory begins at about 43° 37' and 70° 10.3'. The current shown at this position falls between 16 and 22 cm/sec (ave. 19) and flows towards 280°. To obtain the next leg of the trajectory repeat the above calculations in the same manner.

At this point a word of caution is in order. When performing calculations for flows within the channels or for those in the lee of the land the wind has little effect and it is not necessary to include them in the analysis.

ESTIMATION OF OIL TRAJECTORIES

Our present concern is to obtain a first order estimate, as close in real time as possible, for what a particular oil spill trajectory will be, given the location within the study area, tide and local winds. We have already shown in the previous section how it is possible to derive the vector for the surface current and to construct a trajectory progression from one stage of the tide to another. It has also been shown that the tidal currents rather than the non-tidal advective processes are the dominant forces for water transport and how the winds will alter, to some degree, the nature of that tidal flow. Given the presented current data and correction methods we may now consider how spilled oil will move in this environment.

Oil spill behavior has been studied by many authors and there is a large volume of references available on the subject. Among these there is one very thorough review by Stolzenbach (1977) that covers modeling of wind fields and resultant surface stress, advection of oil slicks by waves and currents, oil slick transformations, the results of a few direct observations and a dozen or so different composite prediction models. Another excellent review on the nature of hydrocarbons in the environment with particular attention to sources and sinks has been presented by Card, Aho and Gillespie (1981) as part of their Casco Bay Resources Inventory. Some of the subjects covered are for example: oil spills in Maine, transformations of oil in water, lethal, sublethal and long-term effects of oil on the ecosystem. Both of these references are recommended to the reader and are available in the Bigelow Laboratory/ Department of Marine Resources Library.

After reviewing a large volume of literature and attempting to arrive at a somewhat realistic oil spill prediction strategy that could be applied directly in the field, it has become obvious to this investigator that a) no two authors agree on the correct solution and b) the overall complexity of the Casco Bay system does not lend itself to even a moderately complex modeling scheme. This lack of agreement and unsuitability is a direct result of our poor understanding of some of the basic functions and dynamics responsible for estimating wind drag on oiled surfaces under variable conditions of wind speed, sea surface roughness, alterations of viscosity, and wind-wave interactions. The lack of definitive data to support the proper choice turbulence and dispersion coefficients for systems with variable depth, bottom roughness and length scales is also a problem. These and other related problems of ocean dynamics have concerned oceanographers and mathematicians for the past fifty years and will undoubtedly be the subjects of study for a long time to come.

Given the complexities and uncertainties involved with this problem there is, nevertheless, a general consensus of opinion that for shallow water wind stress conditions for periods lasting between 6 and 100 hours and for length scales of less than 100 km, the movement of oil slicks and patches will be directly downwind at speeds approximately 3-5% of the wind speed. Please keep in mind that these estimates and conclusions reduce a complex problem down to the simplest of terms and are subject to argument.

The above considerations for the movement of slicks does not include the effects of local currents, and corrections for them must be applied before we can arrive at any estimate of an oil spill trajectory.

This is accomplished in the same manner as the procedure previously discussed for the estimation of surface currents in the presence of wind. In this case, wind speeds are converted to cm/sec, multiplied by 5% and the wind direction converted to the direction in which it is blowing towards. This vector is added to that of the local current vector as shown on the current charts already presented to yield the oil trajectory for that given tidal period. The next two hour trajectory period starts at the termination of the previous one and new wind and current values are calculated, if different from those before, and the process is repeated to build series of progressive vector diagrams.

There may arise situations where the wind effects on the movement of the spill will be of such a magnitude that the effect of the local current will be almost completely masked. This may be especially so in offshore waters where current speeds tend to be slower and the fetch of stronger winds is longer. If for example, a spill occurred during an ebbing tide in the vicinity of the eastern end of West Cod Ledge with the wind blowing at 50 kt (2570 cm/sec), from the west the speed of the slick would be about 129 cm/sec (2570 x .05) where the local current is only about 20 cm/sec to the south. Adding these two vectors gives a resultant vector of about 130 cm/sec (2.5 kt) towards 098°. Once an oil spill reaches the open ocean beyond the Casco Bay area it becomes difficult to anticipate just what the net transport would be due to our lack of data on the currents of the Maine coastal shelf. This has been aptly demonstrated in the case of the *Northern Gulf* spill in November of 1963 when 800 thousand gallons of crude were released after the vessel went aground on West Cod Ledge. Much of this spill ended up on the shores near the Bristol-Friendship area which is about 40 miles to the

northeast of Casco Bay. The direction that this spill traveled is contrary to the generally accepted idea of a southwesterly current along the coast and was due primarily to the effect of the winds at the time, together with a suspected slow gyre-like circulation which had an additive effect on the movement.

SUMMARY AND RECOMMENDATIONS

This study has presented much new data on the currents, hydrography and dynamic processes found in the Casco Bay area. It has also been shown that the interrelationships of these various factors is a complex one and that with regards to obtaining definitive solutions for fine scale flow predictions there are no simple answers that will satisfy all conditions. I have nevertheless attempted to provide some practical information for real time for oil spill trajectory estimation given certain conditions. This has been presented with the realization that the demonstrated variabilities within the system may alter the outcome of those estimates.

Considering the rest of the coast of Maine beyond the Casco Bay area with its many islands, bays and estuaries and our general lack of information about the currents and hydrographic characteristics specific to those areas it is suggested that the State consider plans to acquire such information not only for oil spill response purposes but for the support of fisheries research, planning of industrial development and offshore dumping and dredging activities and for general marine safety purposes including search and rescue.

Finally the best strategy for dealing with the potential for oil spills is that of prior prevention. One practical solution to minimize

the chances that a spill or any other shipping accident might occur has been put into operation by the port of San Francisco, California. This system is a dedicated marine traffic control center which is responsible for the routing and scheduling of all ships entering that port. It operates in the same fashion as an aircraft control tower with the addition that all ships and the center communicate on the same frequency in the open channel mode. In this manner any captain operating in the area is constantly apprised of the movements and intentions of all other ships which may be in conflict with his. The center also informs all ships of up-to-date local weather, oceanic conditions and near-by ship locations (by tracking radar) and has the authority to intervene in the flow of traffic if conditions warrant such action. Given the potential, present and future, for hazardous situations arising for ships approaching Portland Harbor, a similar or scaled down version of the San Francisco traffic control system might well be considered for the Casco Bay region.

REFERENCES

Card, D.J., R.A. Aho and L.M. Gillespie (1981) Casco Bay Coastal Resources Inventory. State of Maine Department of Marine Resources Fisheries Research Laboratory, West Boothbay Harbor, Maine.

Garside, C., T.C. Malone, O.A. Roels and F.A. Sharfstein (1976) An evaluation of sewage-derived nutrients and their influences on the Hudson estuary and New York Bight. *Estuar. Coast. Mar. Sci.* 4: 281-289.

Stolzenbach, K.D., O.S. Madsen, E.E. Adams, A.M. Pollack and C.K. Cooper (1977) A Review and Evaluation of Basic Techniques for Predicting the Behavior of Surface Oil Slicks. Massachusetts Institute of Technology Report No. MITSG 77-8, March 1977.

Thorade, H. (1914) Die Geschwindigkeit von Triftströmungen und die Ekman'sche Theorie. *Ann. d. Hydr. u. Marit. Meteorol.*, Vol. 42, p. 379.

Witting, R. (1909) Zur Kenntnis des vom Winde erzeugten Oberflächen-stromes. *Ann. d. Hydr. u. Marit. Meteorol.*, Vol. 37, p. 193.

Yentsch, C.S. and D.W. Menzel (1963) A method for the determination of plankton chlorophyll and phaeophytin by fluorescence. *Deep-Sea Res.* 10: 221-231.

LIST OF FIGURES

NORTHWESTERN GULF OF MAINE

Figure 2. The Casco Bay region.

Figure 3. Location of hydrographic station positions for August/September
1980.

Radar
Reflector

ID
Flags

A

B

1/2"x 3'
Conduit Mast

1/2"x 8' Conduit Mast

1/2"x24"x 24"
plywood &
styrofoam
float

1/2"x 18"x 18"
plywood &
styrofoam float

pipe
clamps

Ballast

1/4"x 6"chain

Ballast

2 - 24"x 24"
crossed plywood
panels

SURFACE DROGUE

5' to 50' of
1/2" plastic rope

ring

rope bridle

DEEP DROGUE

steel spreader bar
10'x 12'

Rienforced Plastic
Tarp

CURRENT

weighted steel ballast
bar

Figure 4. Surface and deep current measuring drogues.

SURFACE

3 - 9"ALUM. NET FLOATS

CURRENT METER

swivels

8'

10'

10'

20'-1/4" POLYCOATED S.S.CABLE

5'-1/2"CHAIN

4 - 15 lbs. RADIATOR SECTIONS

75'-1/2" poly

25' - 1/2" nylon

100' ea. 1/2" POLY

1 - 15 lbs. RADIATOR SECTION ea.

1 - 9" ALUM. NET FLOAT

10'- 3/8" ea POLYPROPYLENE

Figure 5. Bottom current meter deployment system.

Figure 6. Location of bottom current meter stations. Numbered stations –

Figure 7. Casco Bay area subdivisions.

Figure 8. Casco Bay bottom topography. Non-blackened areas are depths
greater than 10 meters.
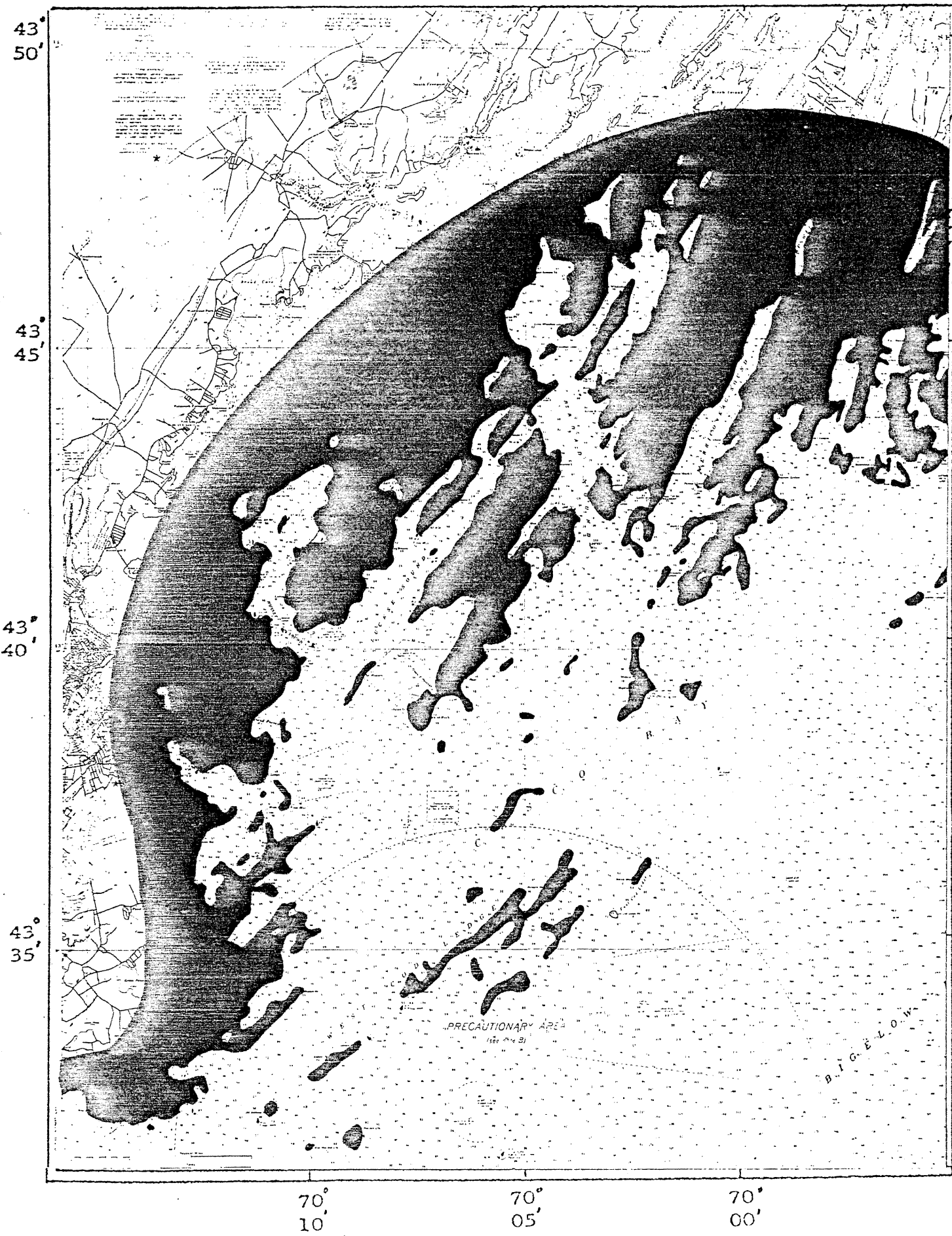
Figure 9. Casco Bay bottom topography. Non-blackened areas are depths greater than 15 meters.
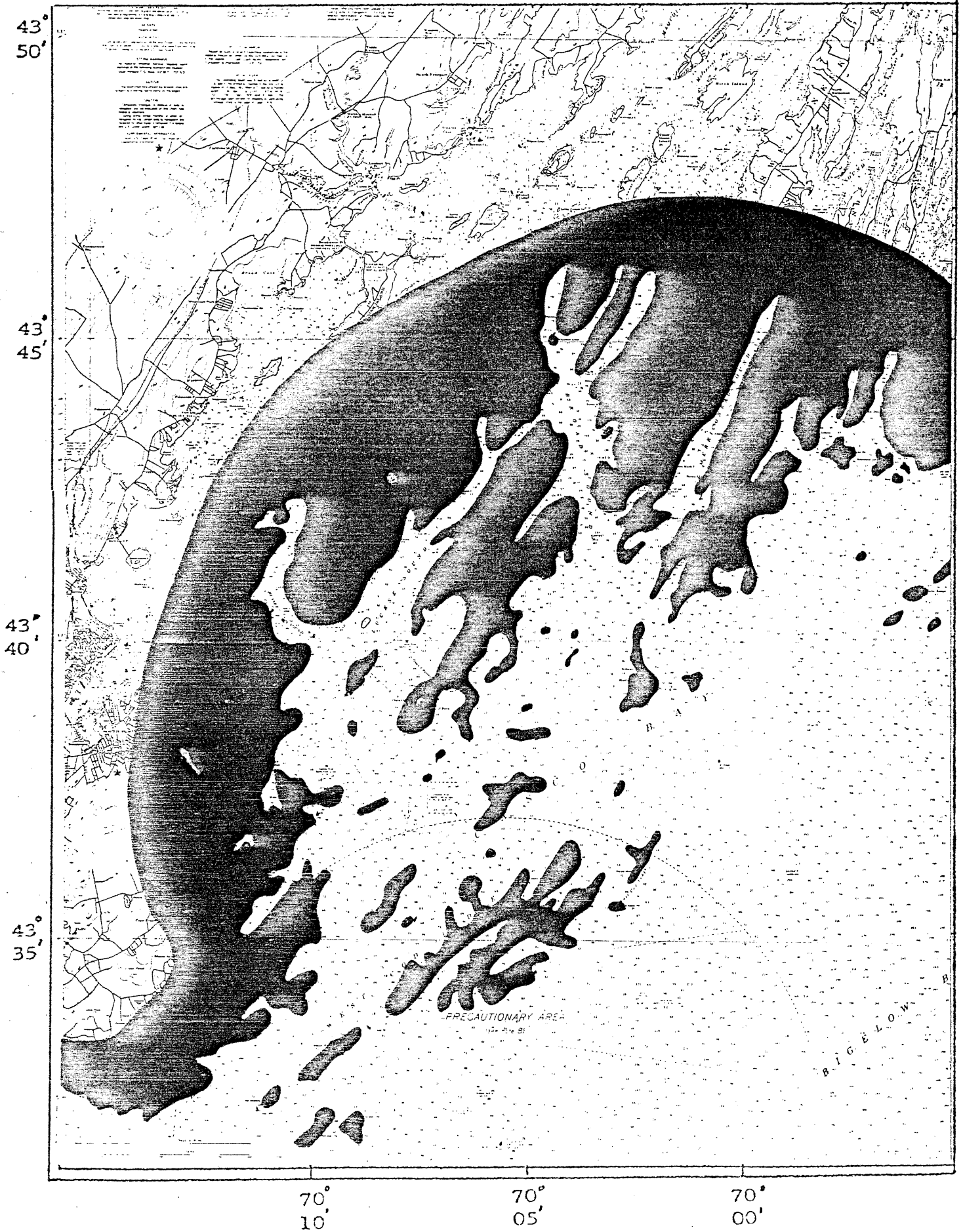
Figure 10. Casco Bay bottom topography. Non-blackened areas are depths
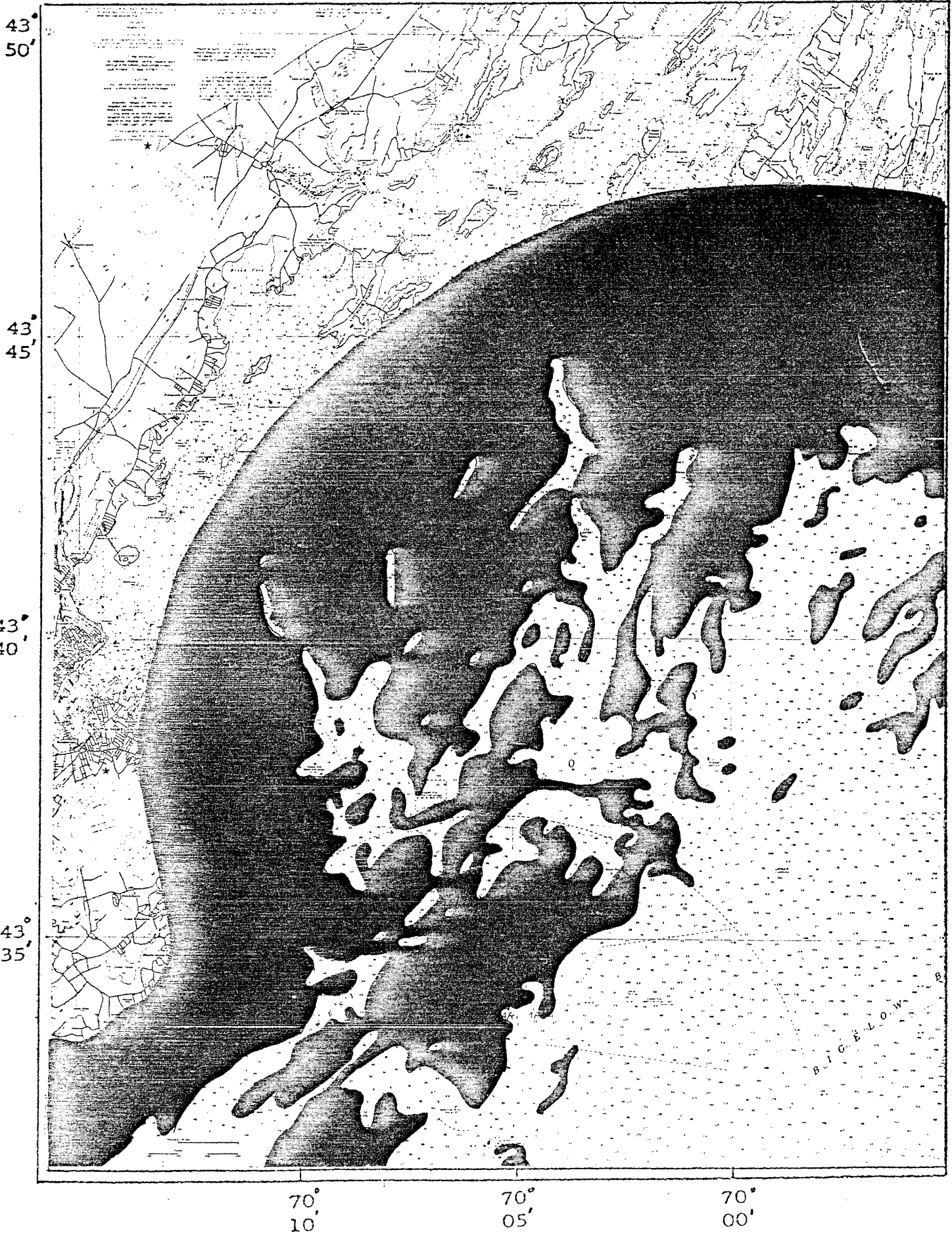
Figure 11. Casco Bay bottom topography. Non-blackened areas are depths

greater than 30 meters.
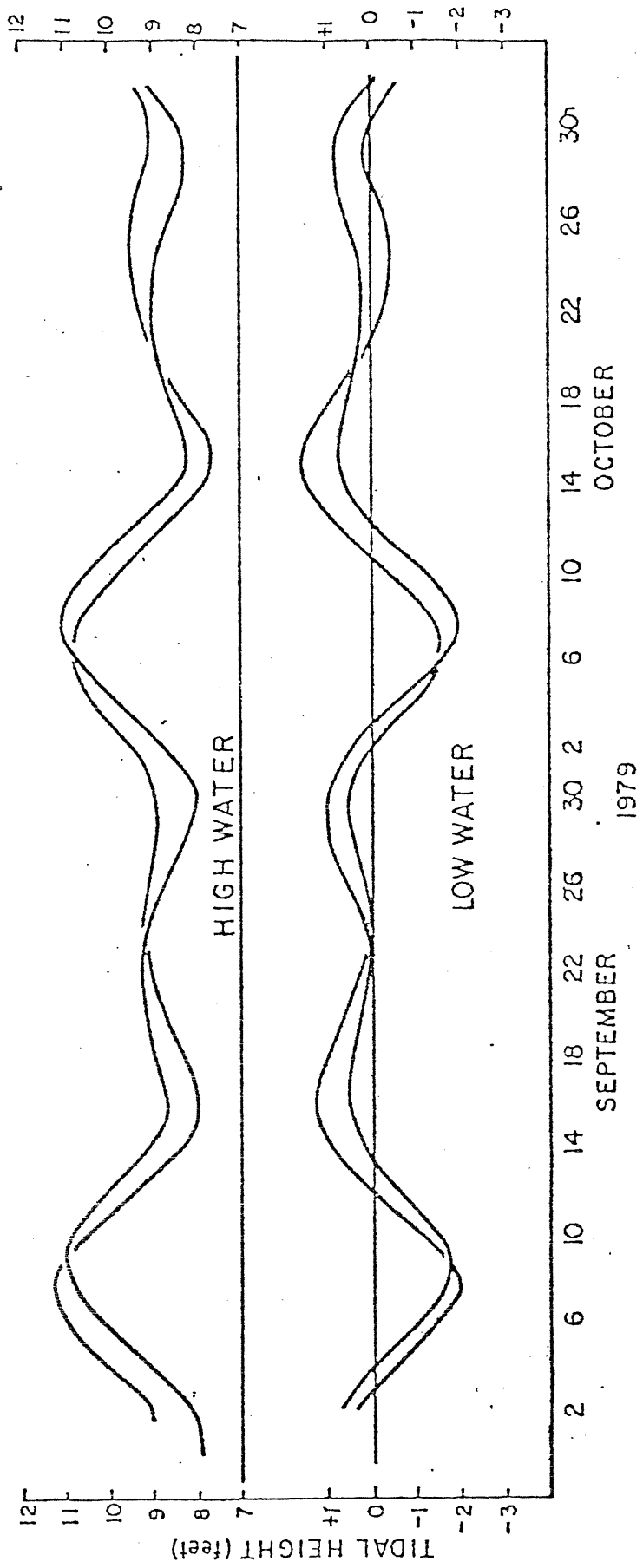
Figure 12. Tidal heights for Portland Harbor, September/October 1979.
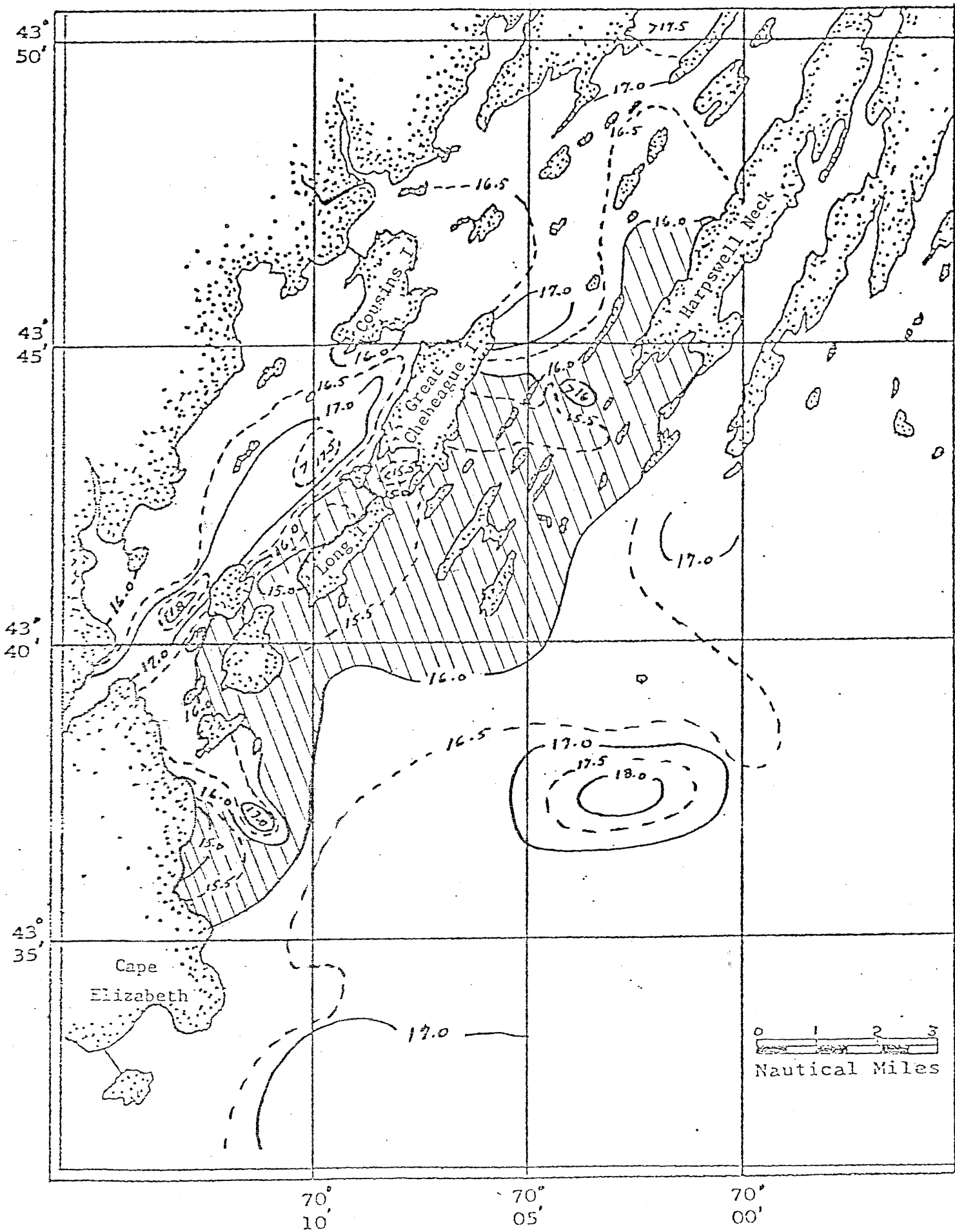
Figure 13.   Surface temperature (°C), ebb tide, August/September 1980.
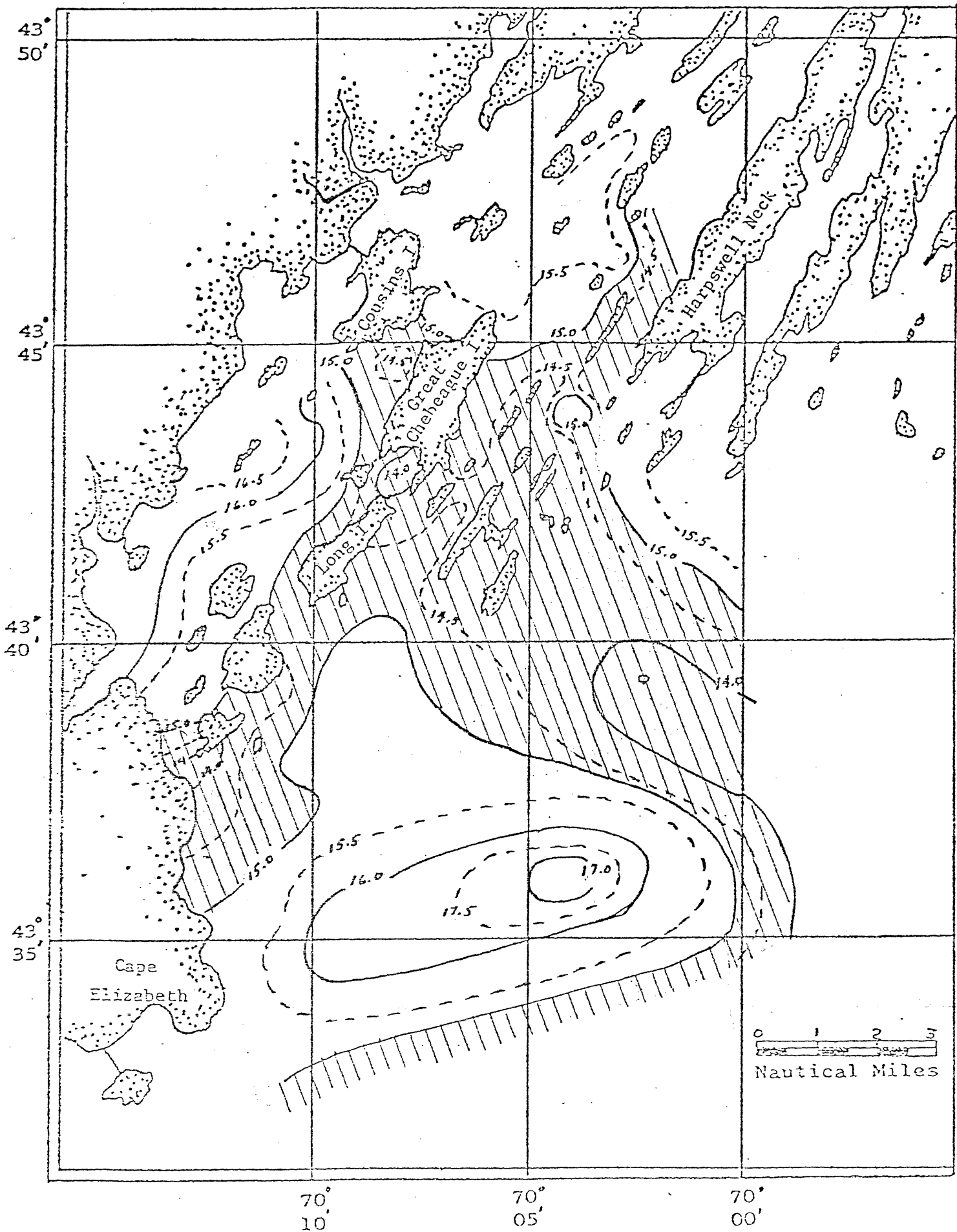
Figure 14.   Temperature ($^\circ$C) at 5 meters, ebb tide, August/September 1980.
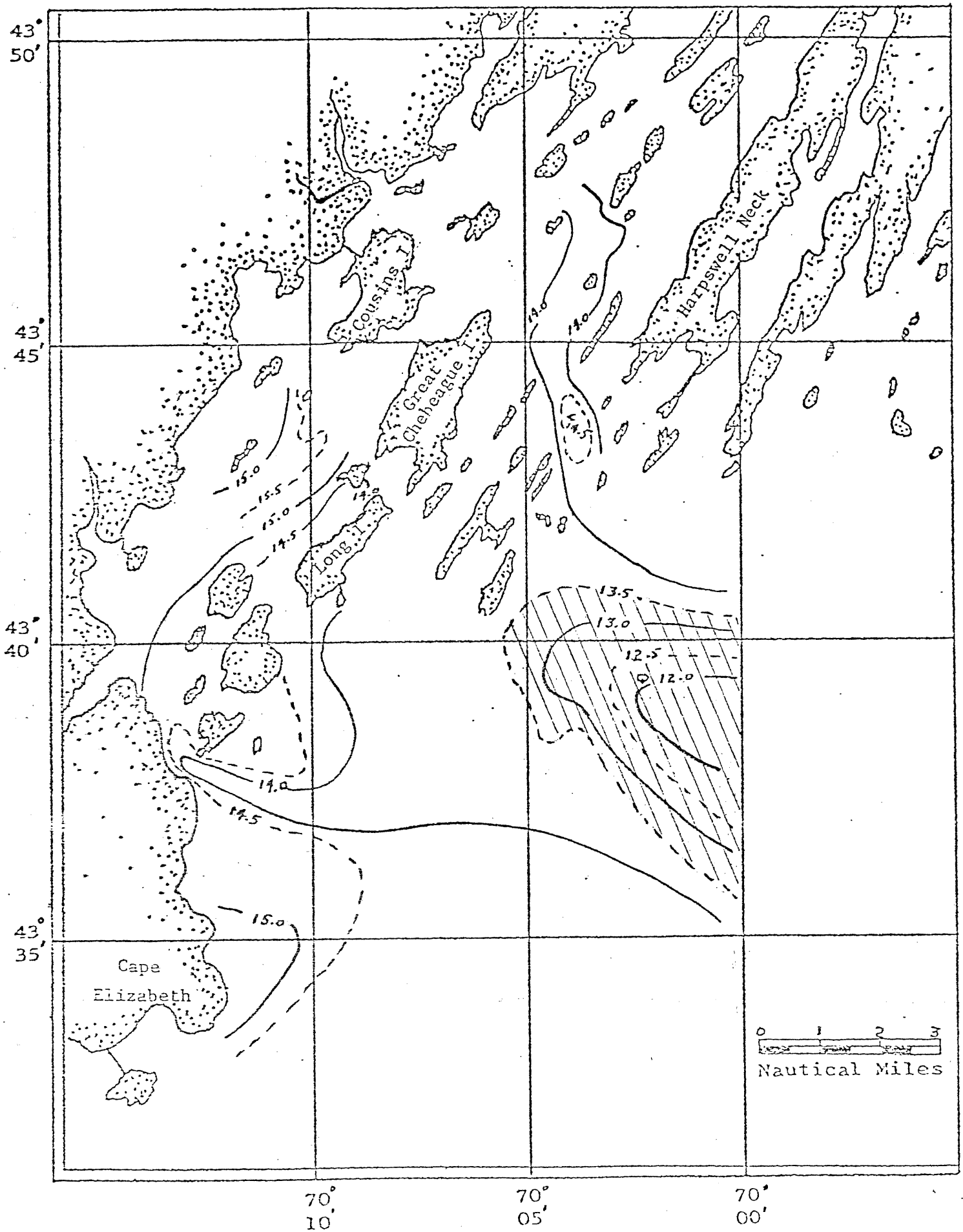
Figure 15.   Temperature ($^{\circ}$C) at 10 meters, ebb tide, August/September 1980.
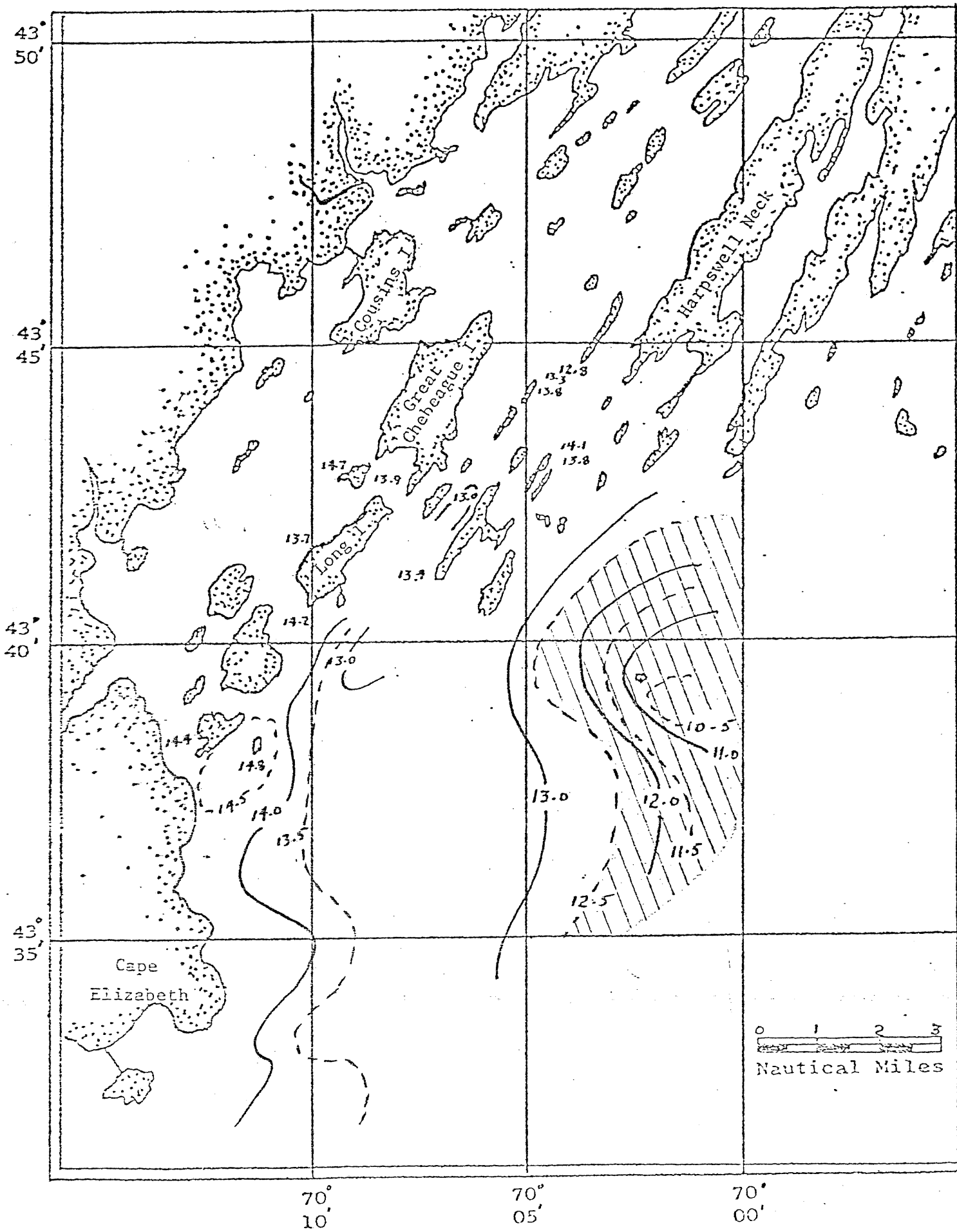
Figure 16.   Temperature ($^{\circ}$C) at 15 meters, ebb tide, August/September 1980.
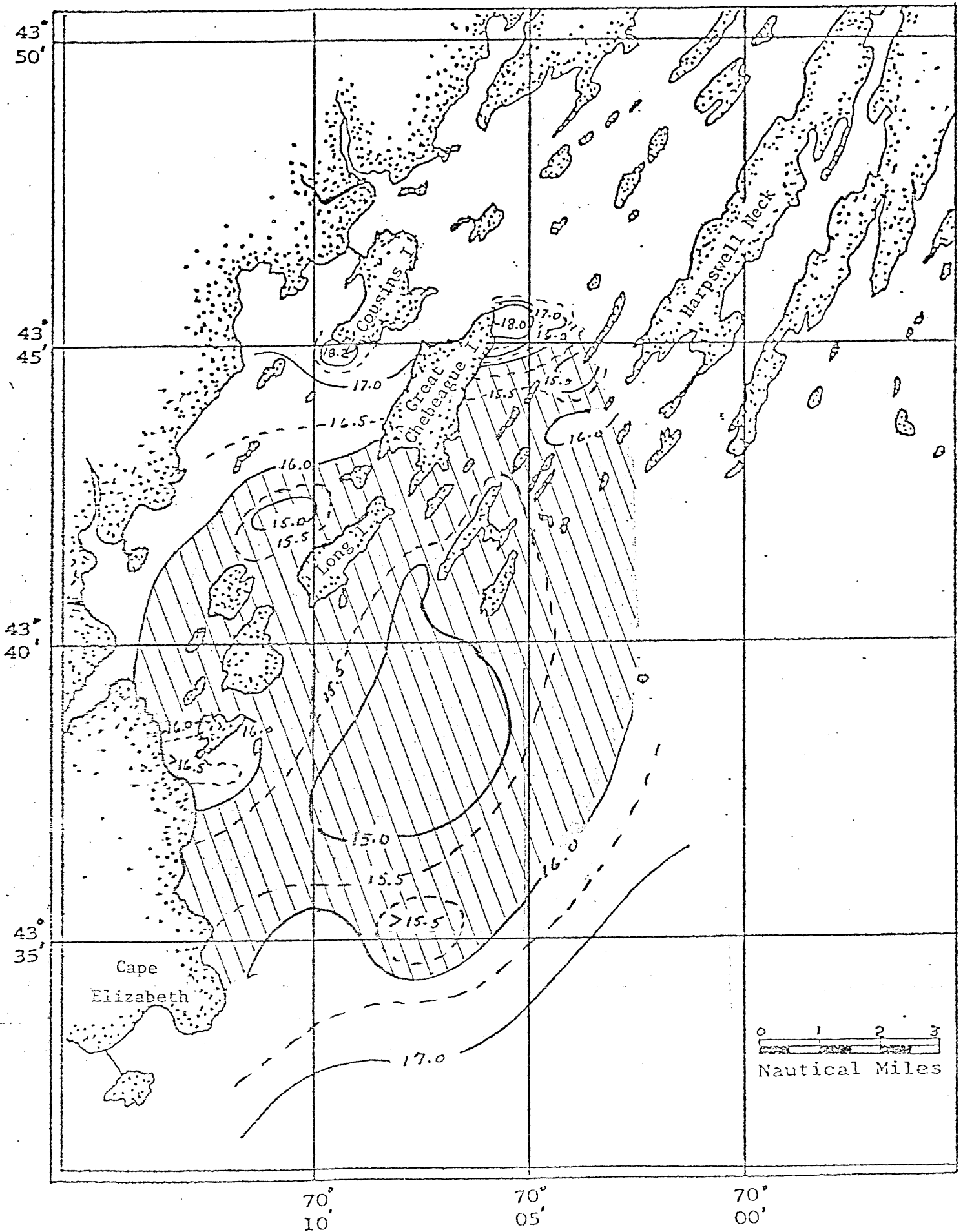
Figure 17. Surface temperature (^{o}C), flood tide, August/September 1980.
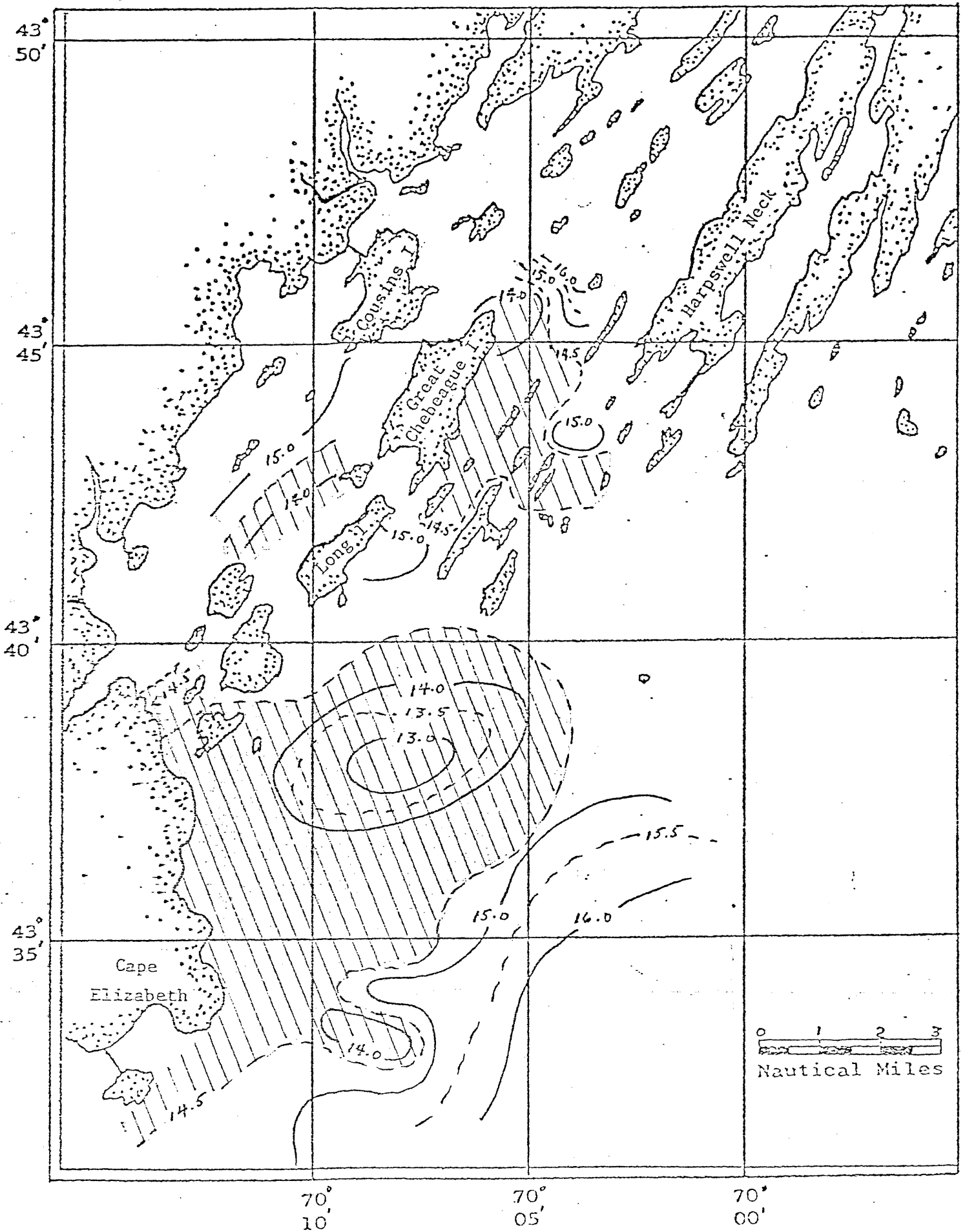
Figure 18.   Temperature ($^{\circ}$C) at 5 meters, flood tide, August/September 1980.
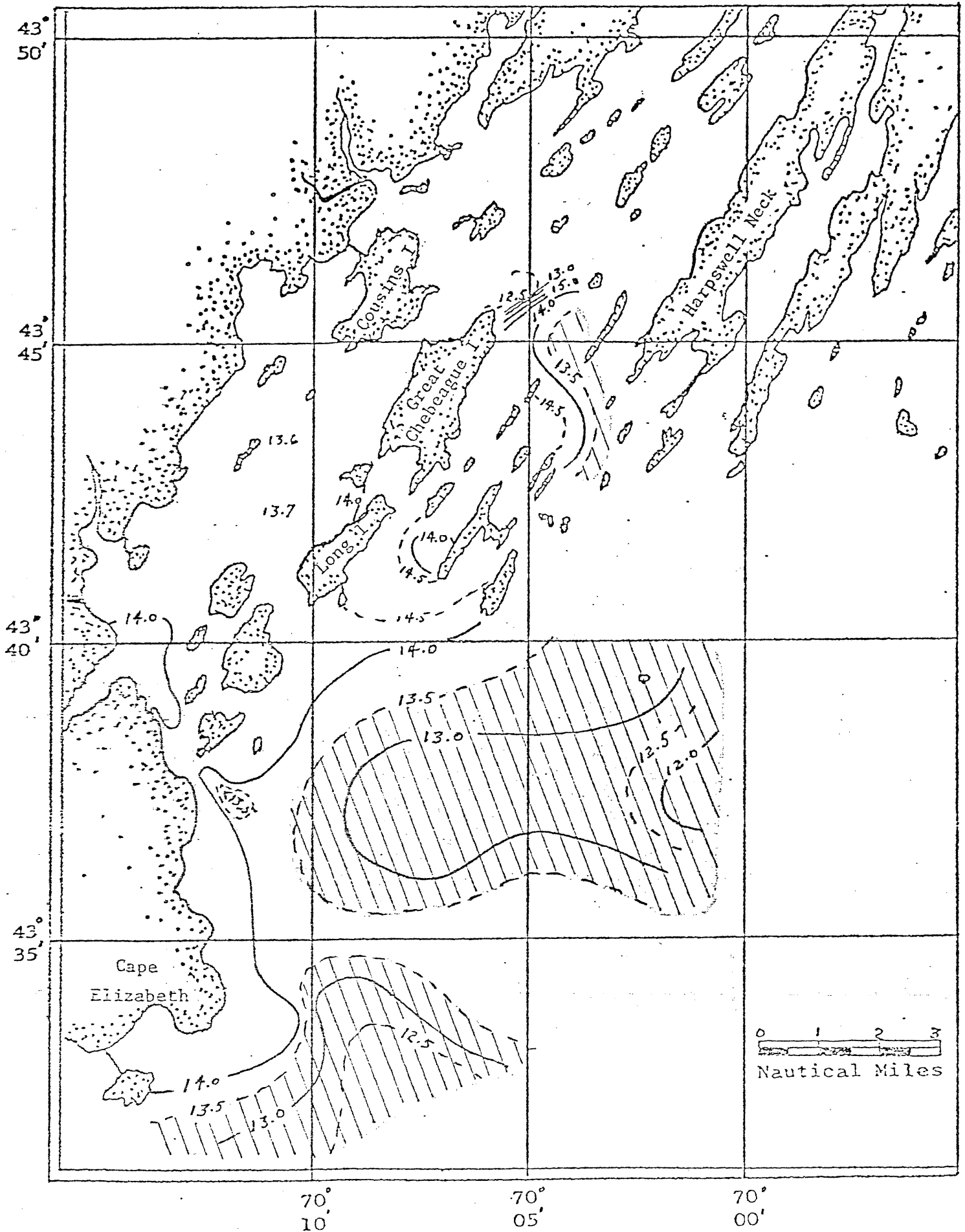
Figure 19. Temperature (^{o}C) at 10 meters, flood tide, August/September 1980.
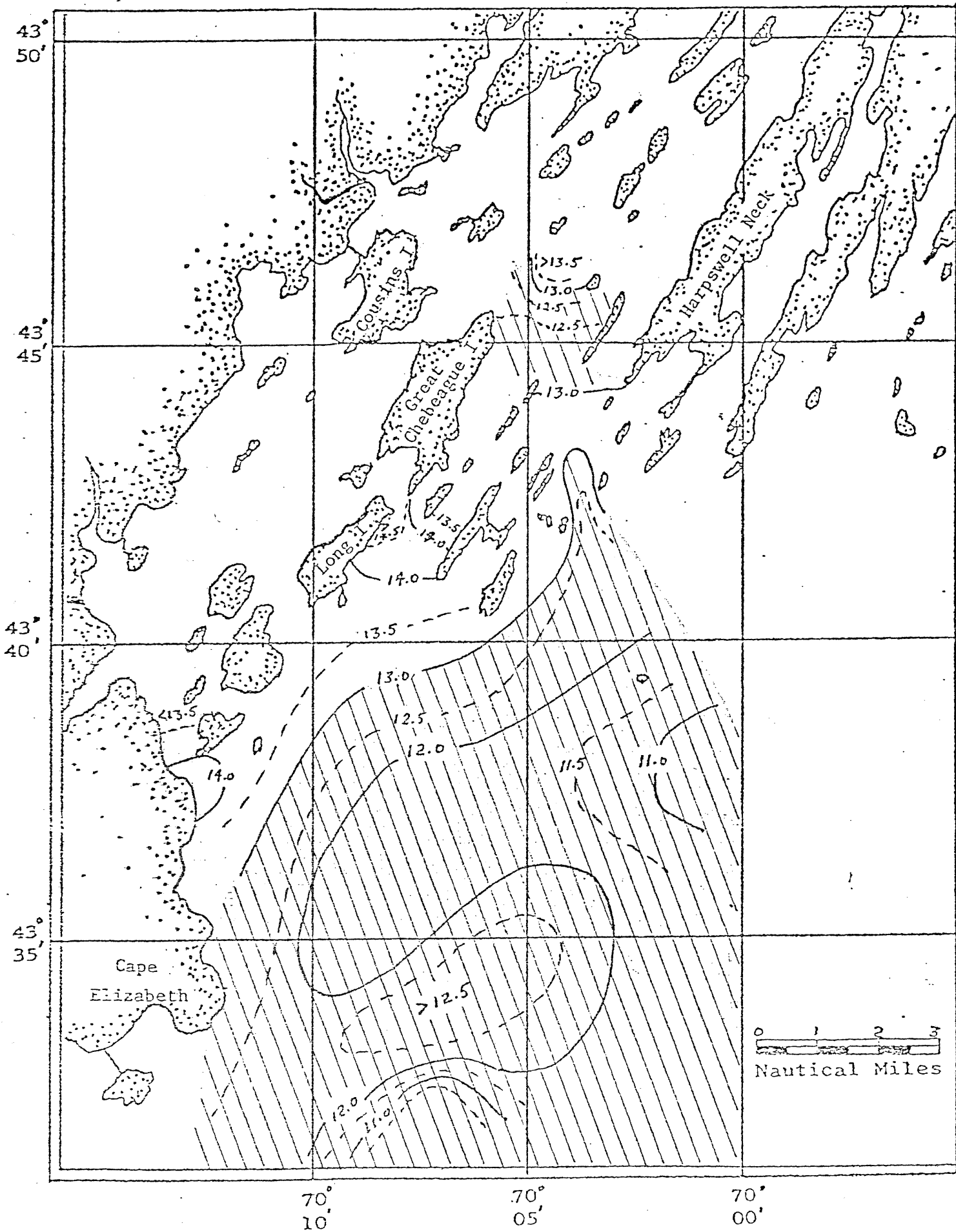
Figure 20. Temperature (°C) at 15 meters, flood tide, August/September 1980.
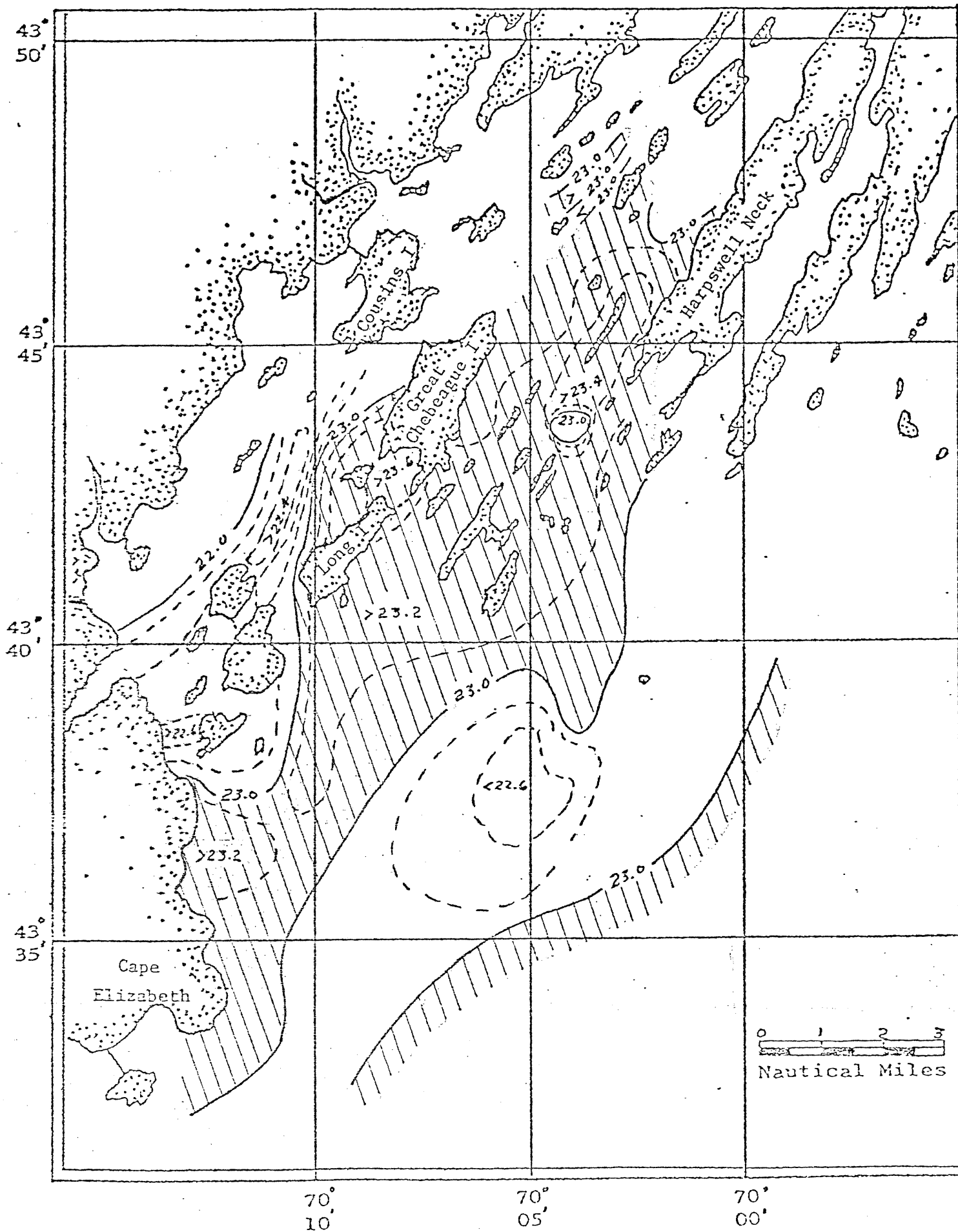
Figure 21. Surface density (σt), ebb tide, August/September 1980.
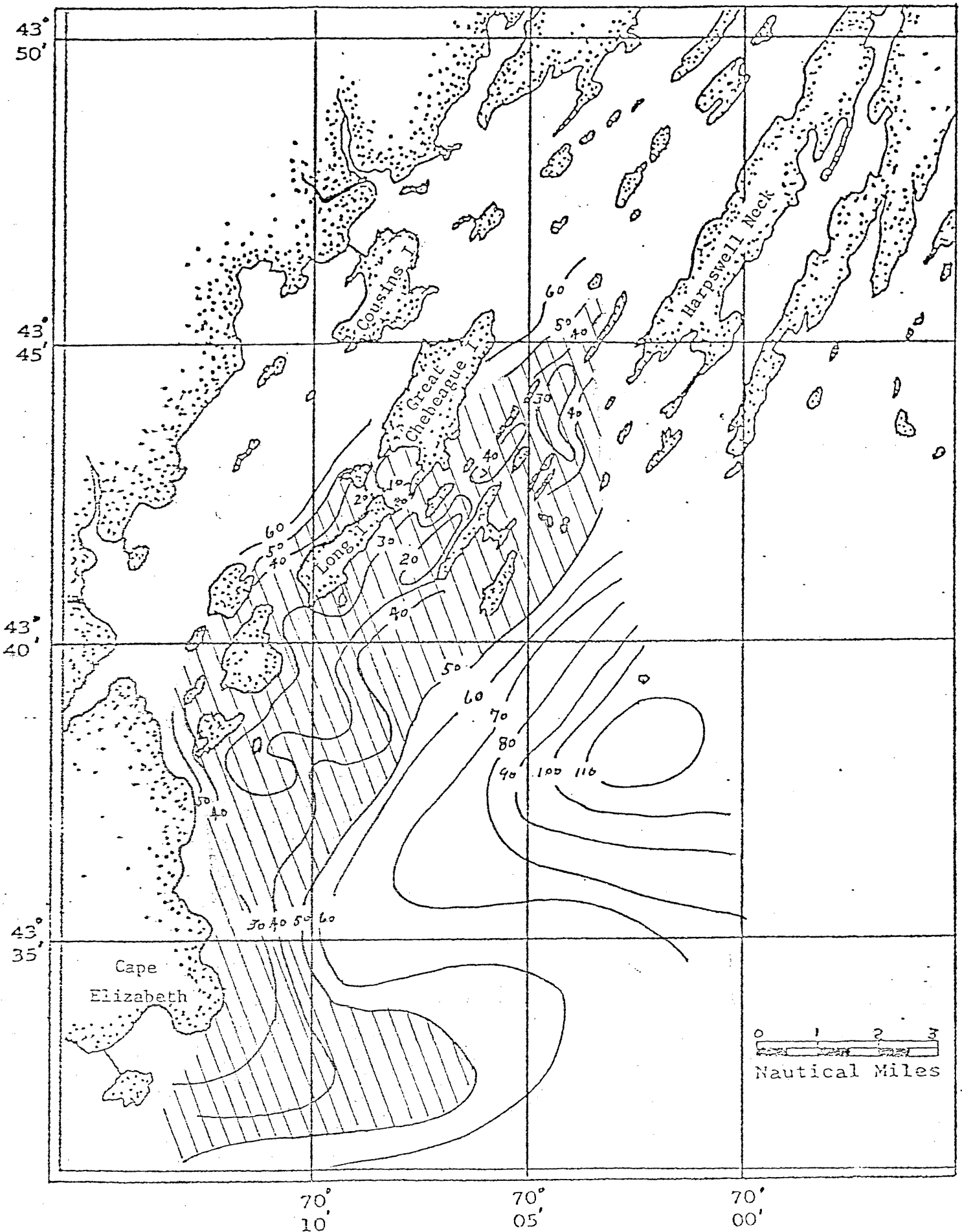
Figure 22. Vertical stability (gm/cm^2/sec x 10^3), 0-15 meters, ebb tide,
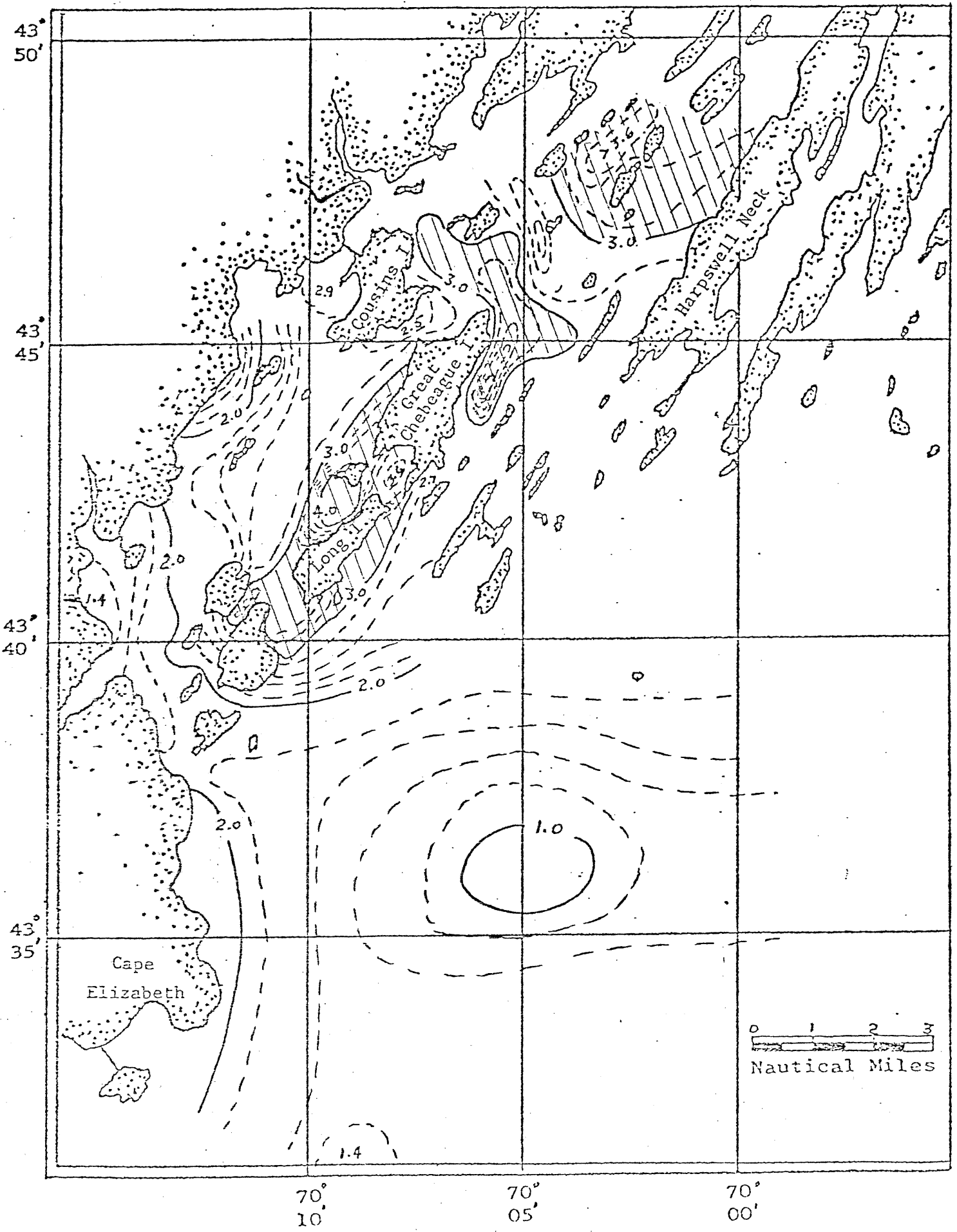
Figure 23. Surface chlorophyll-a (μg-at ℓ^{-1}), ebb tide, August/September
1980
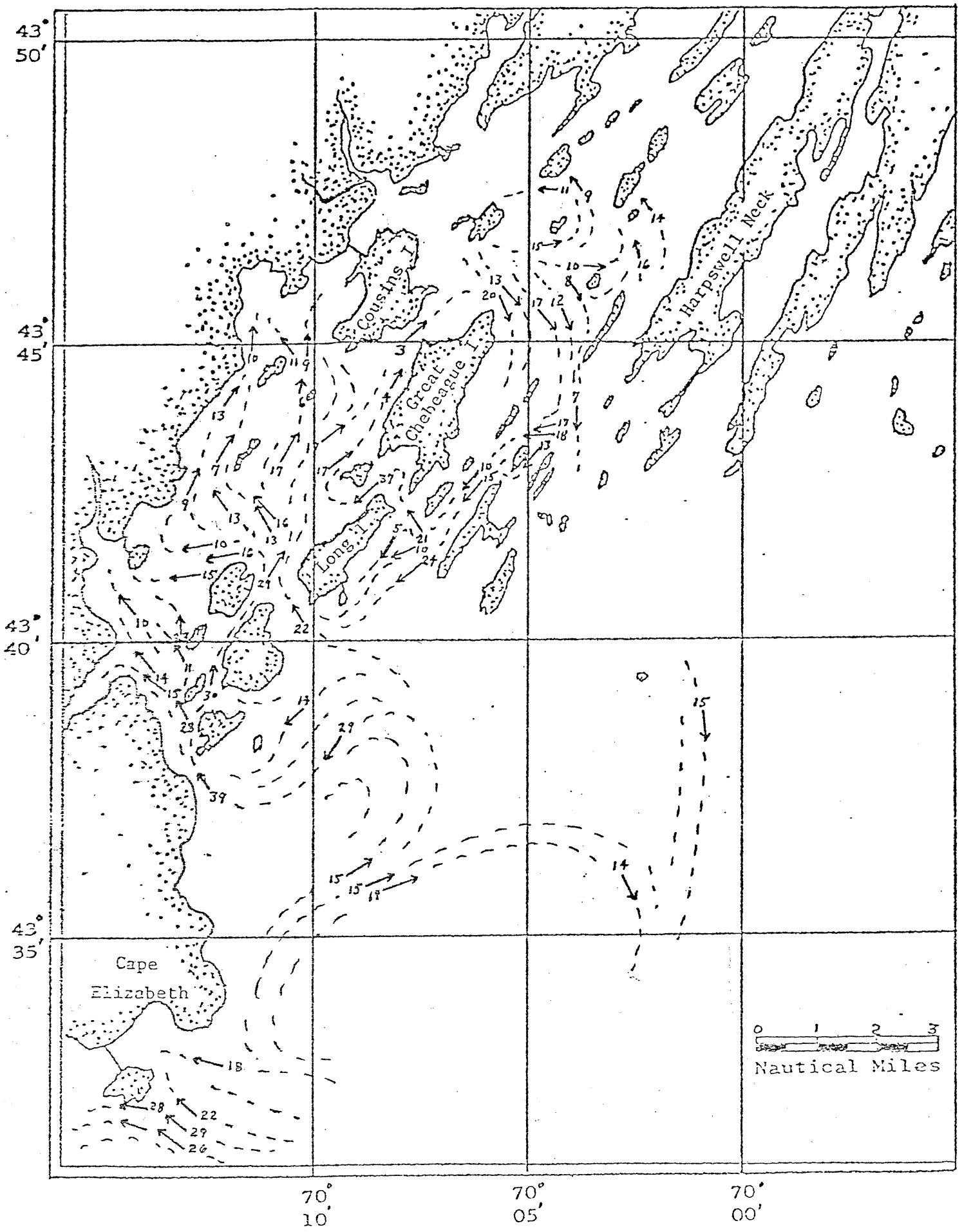
Figure 24. Surface currents for two hour flood tide period L0-L2.
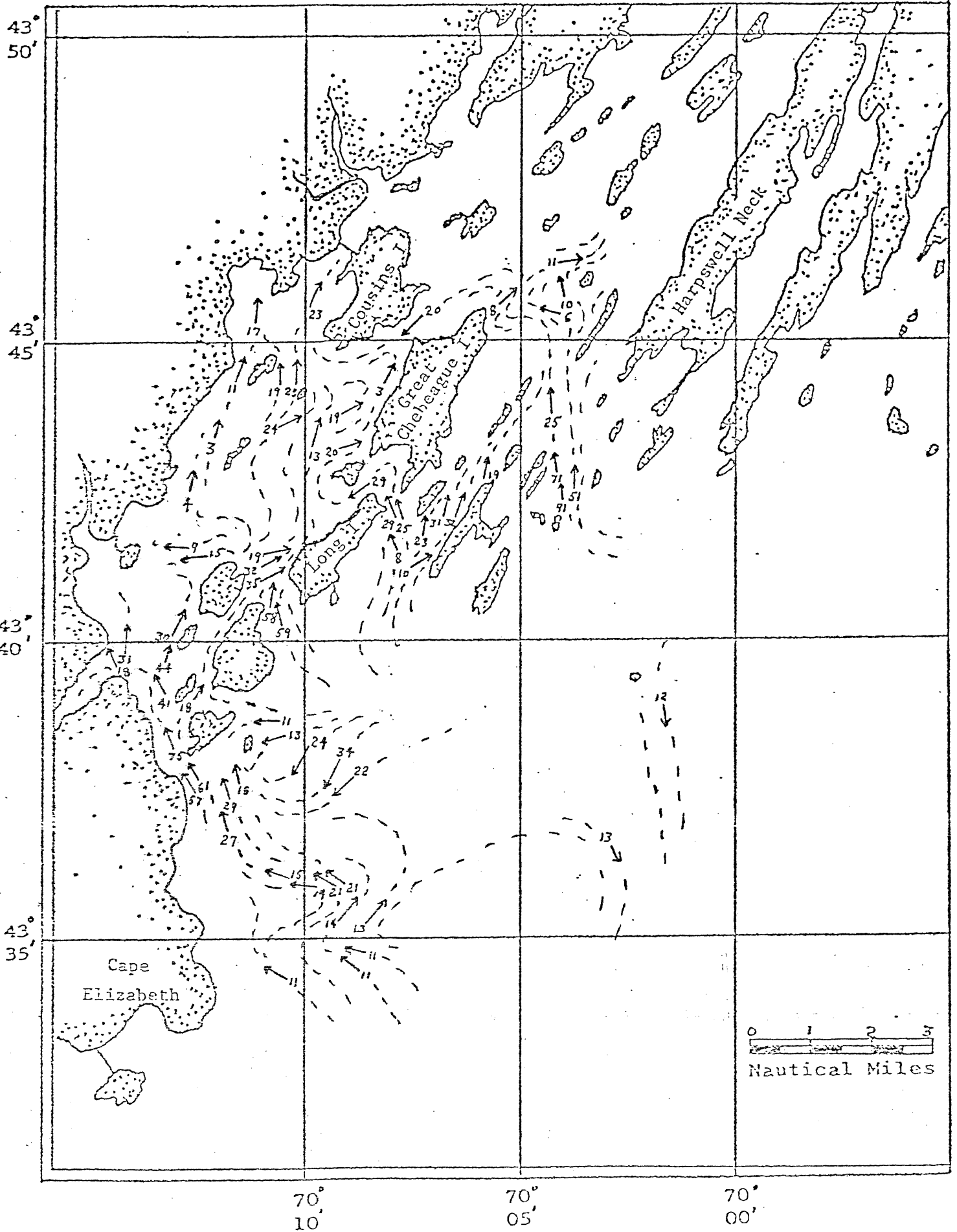
Figure 25. Surface currents for two hour flood tide period L2-L4.
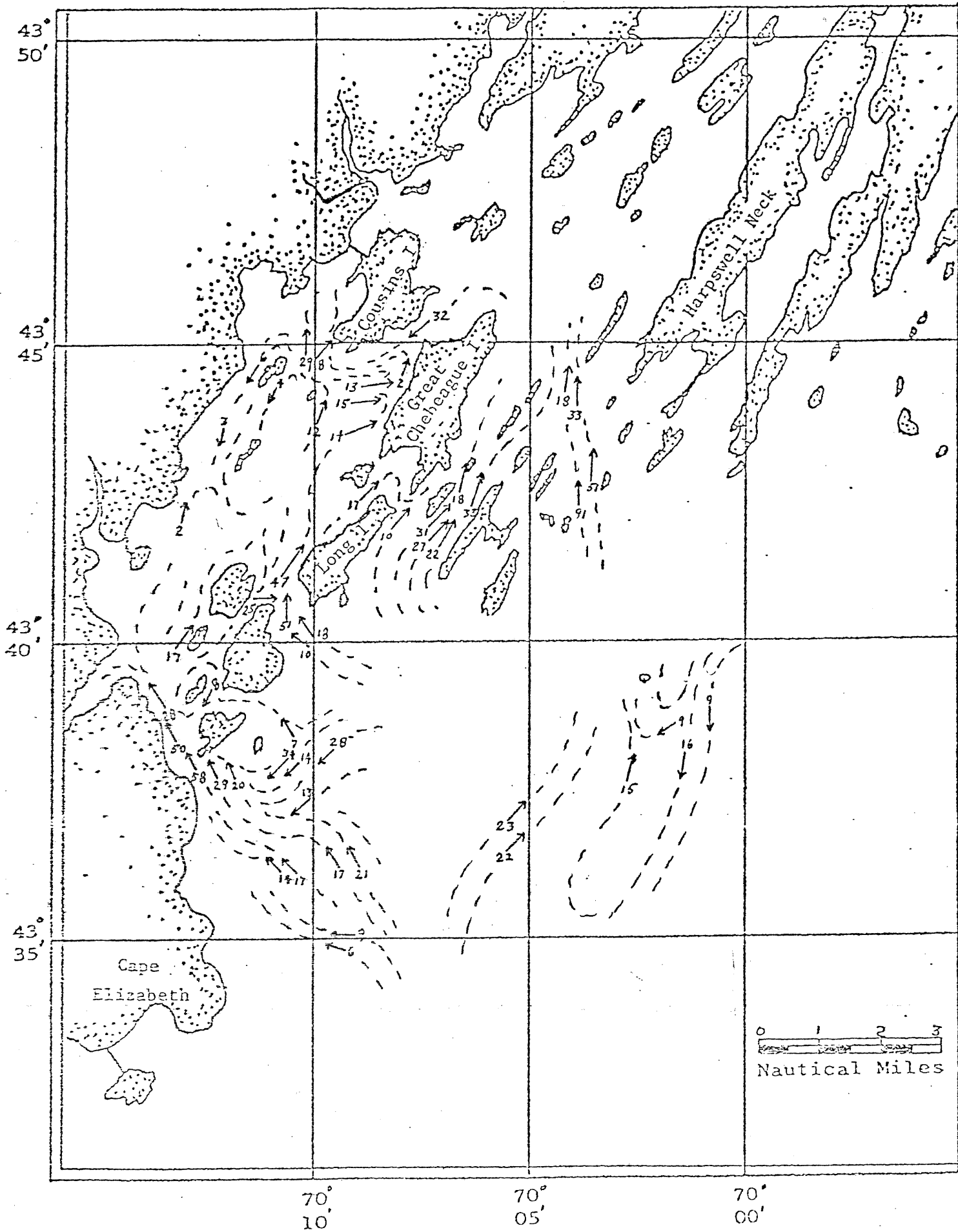
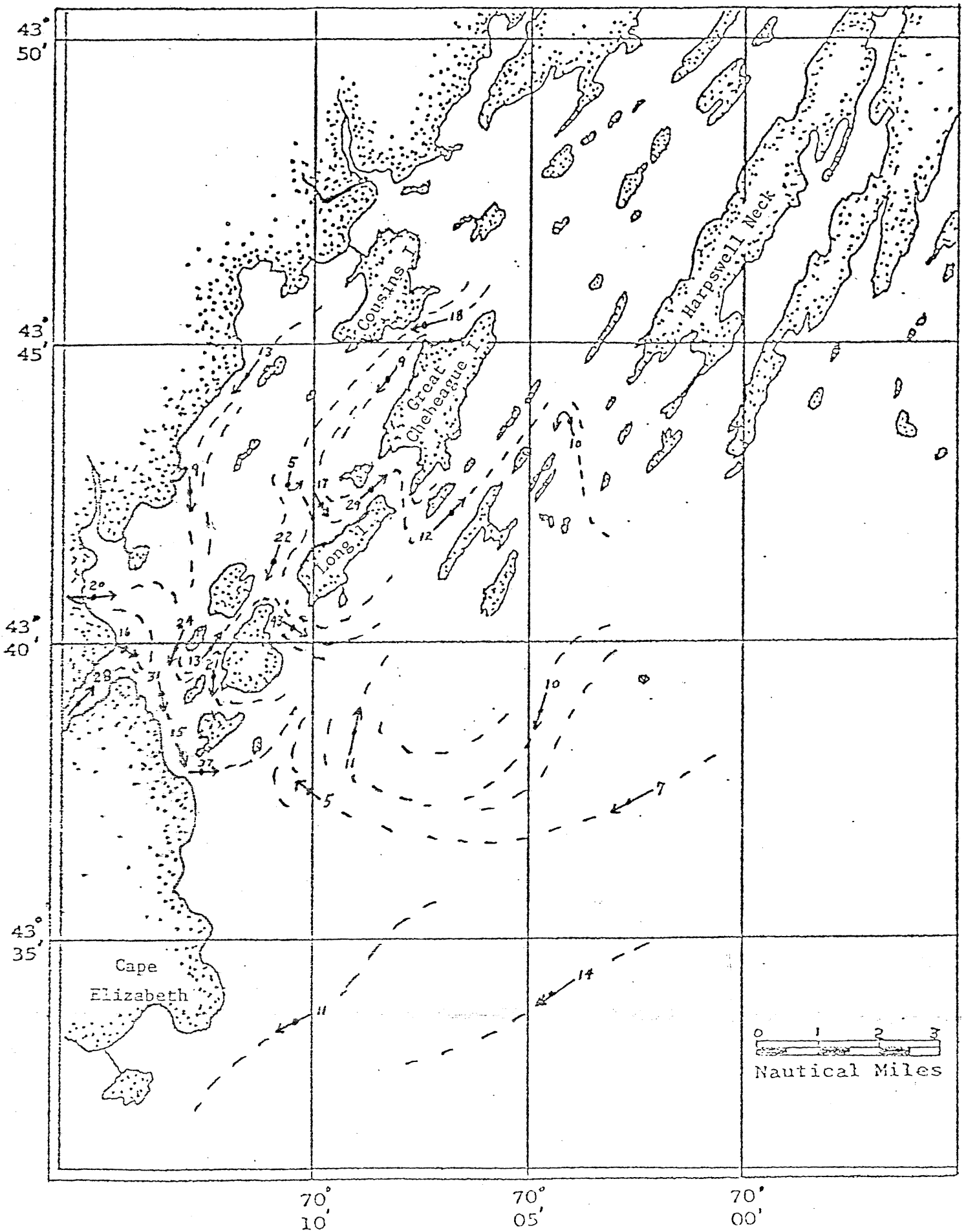Figure 26.   Surface currents for two hour flood tide period L4-H0.
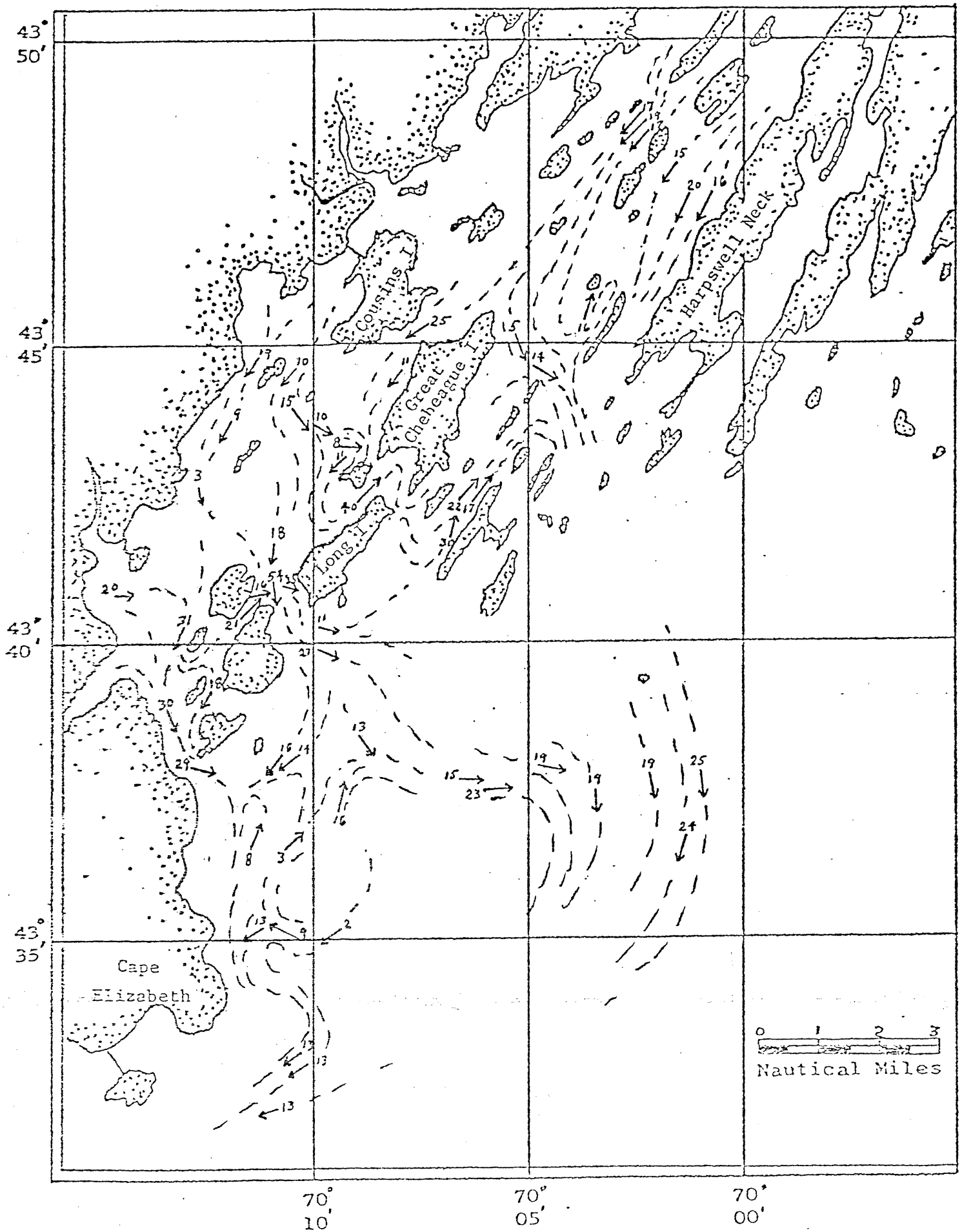
Figure 27. Surface currents for two hour ebb tide period H0-H2.
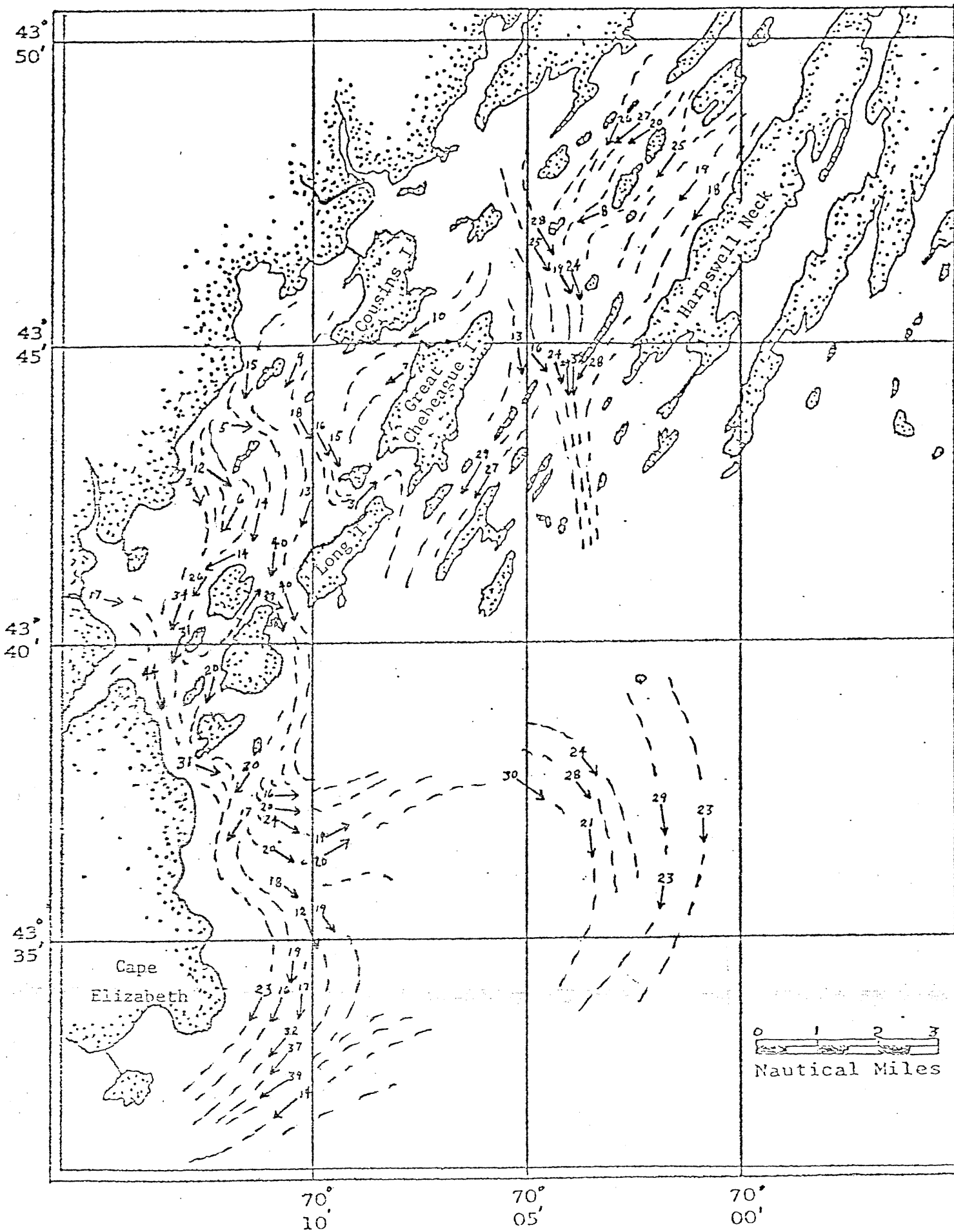
Figure 28. Surface currents for two hour ebb tide period H2-H4.
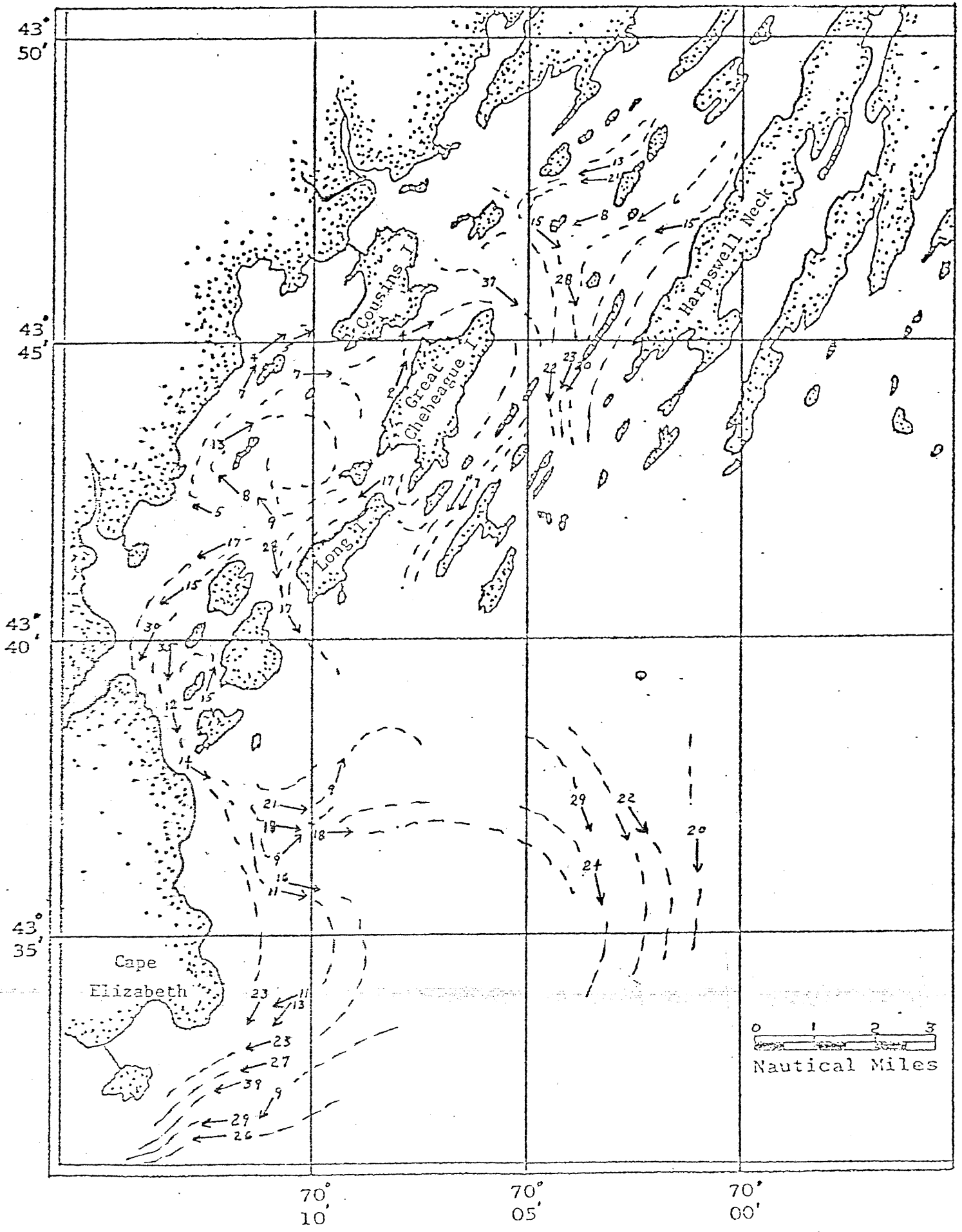
Figure 29. Surface currents for two hour ebb tide period H4-L0.
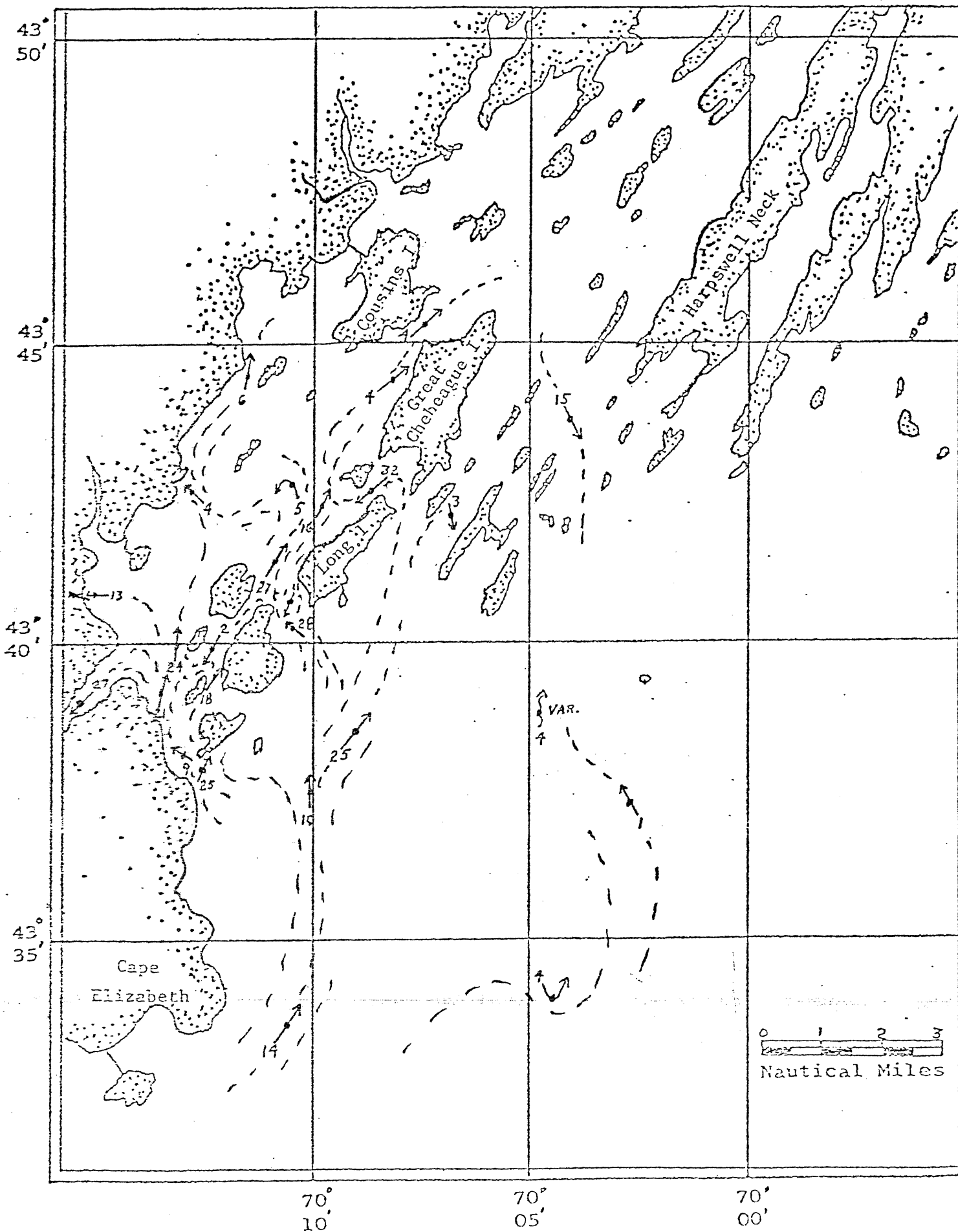
Figure 30. Bottom currents for two hour flood tide period L0-L2.
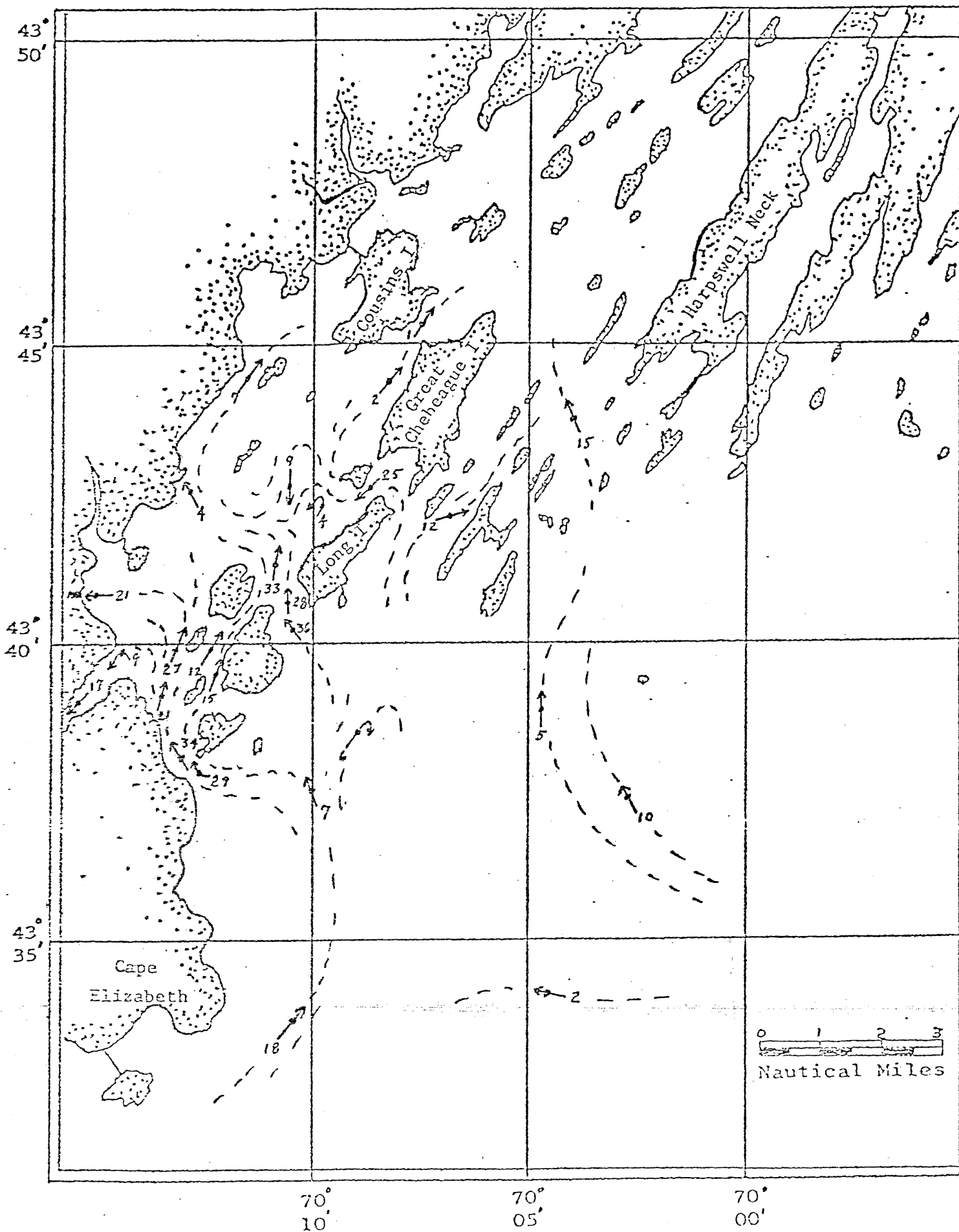
Figure 31. Bottom currents for two hour flood tide period L2-L4.
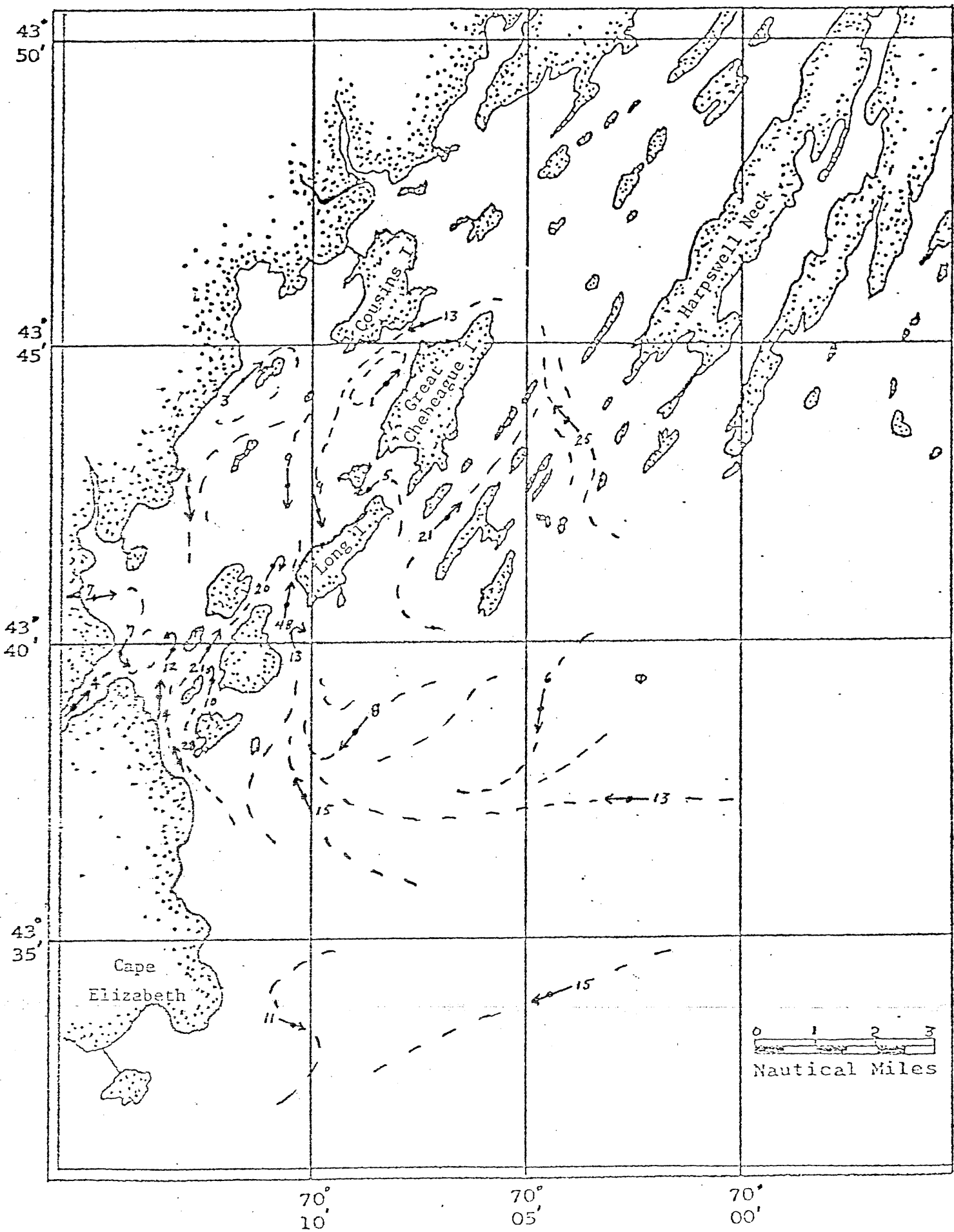
Figure 32. Bottom currents for two hour flood tide period L4-HO.

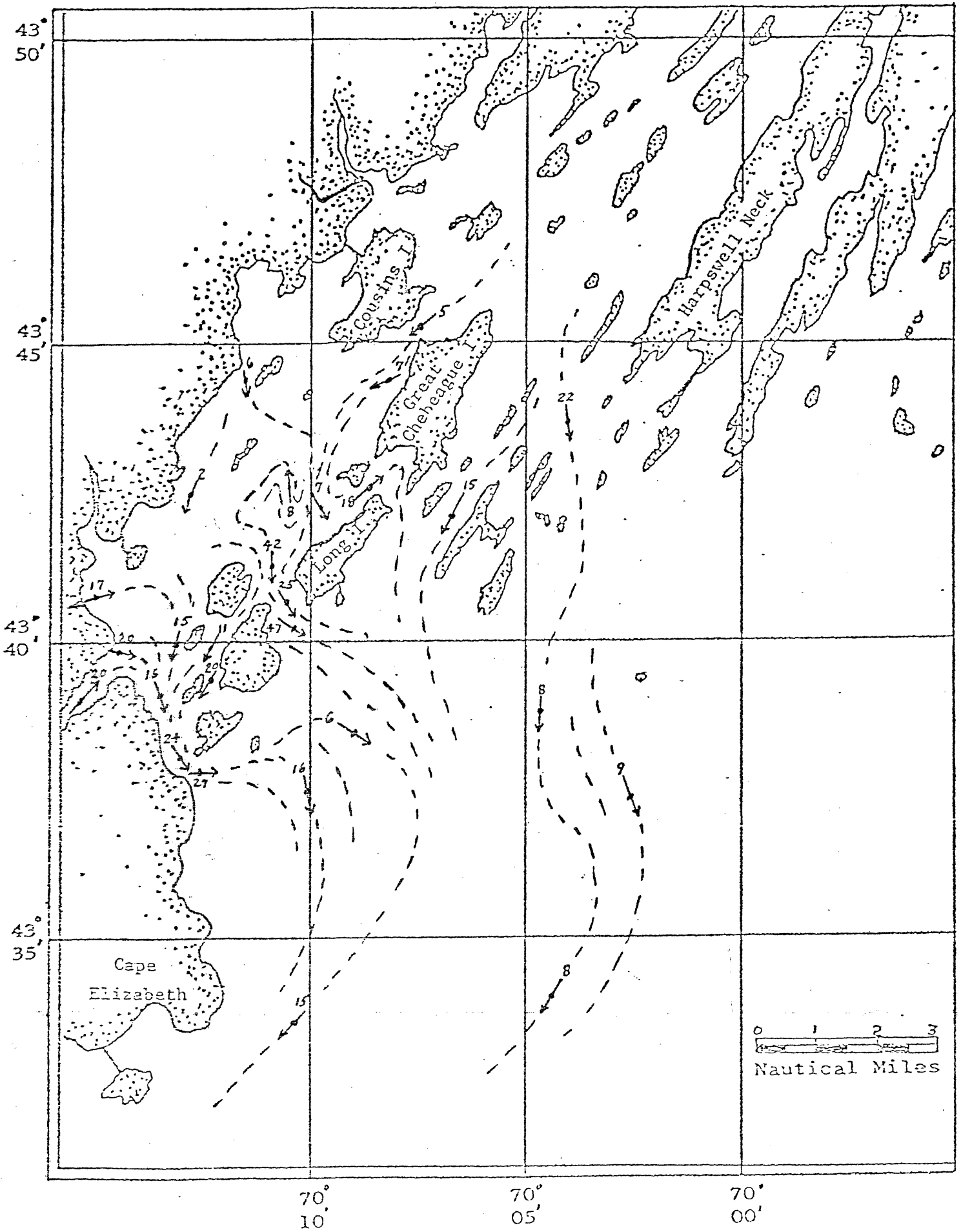Figure 33. Bottom currents for two hour ebb tide period H0-H2.

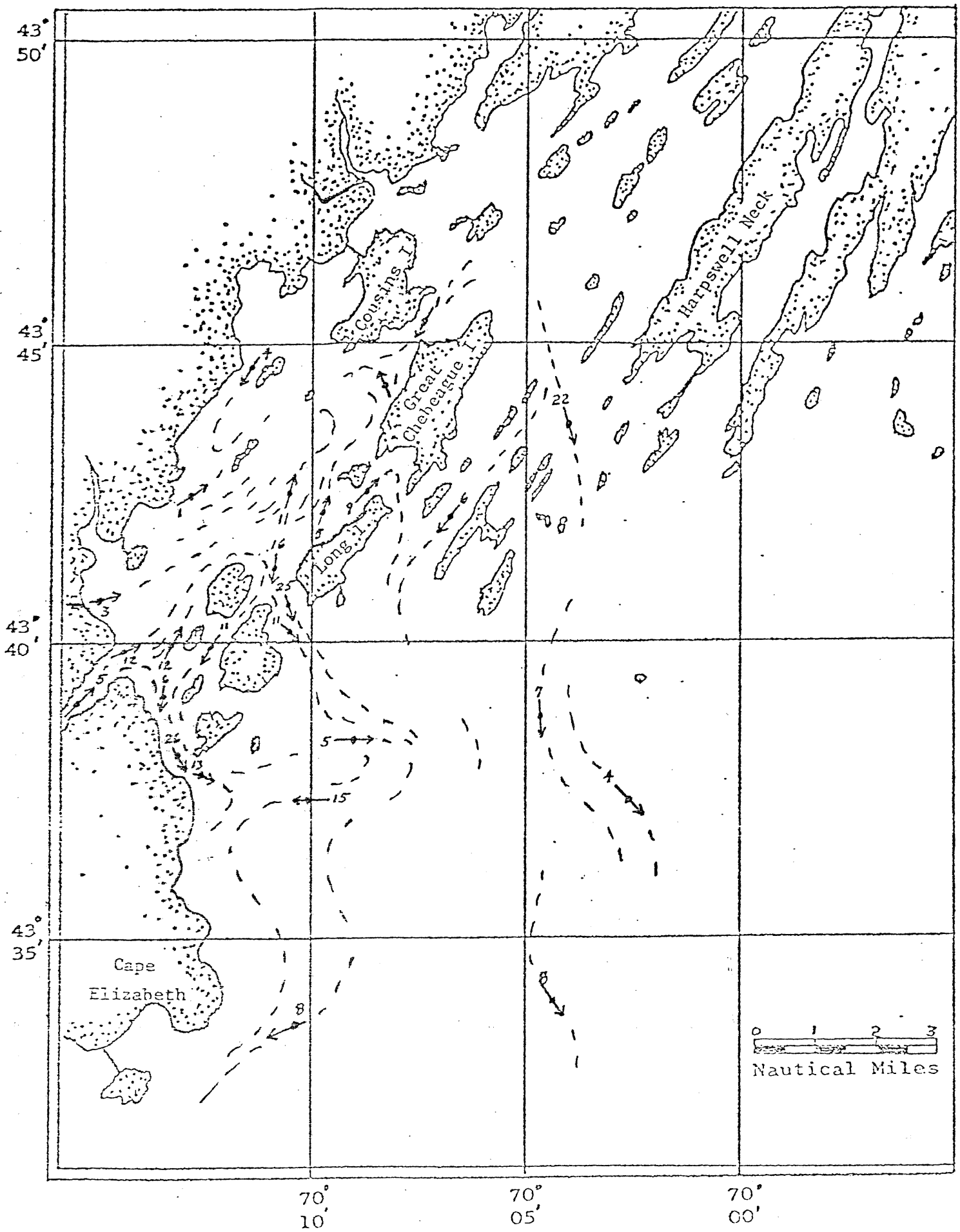Figure 34. Bottom currents for two hour ebb tide period H2-H4.

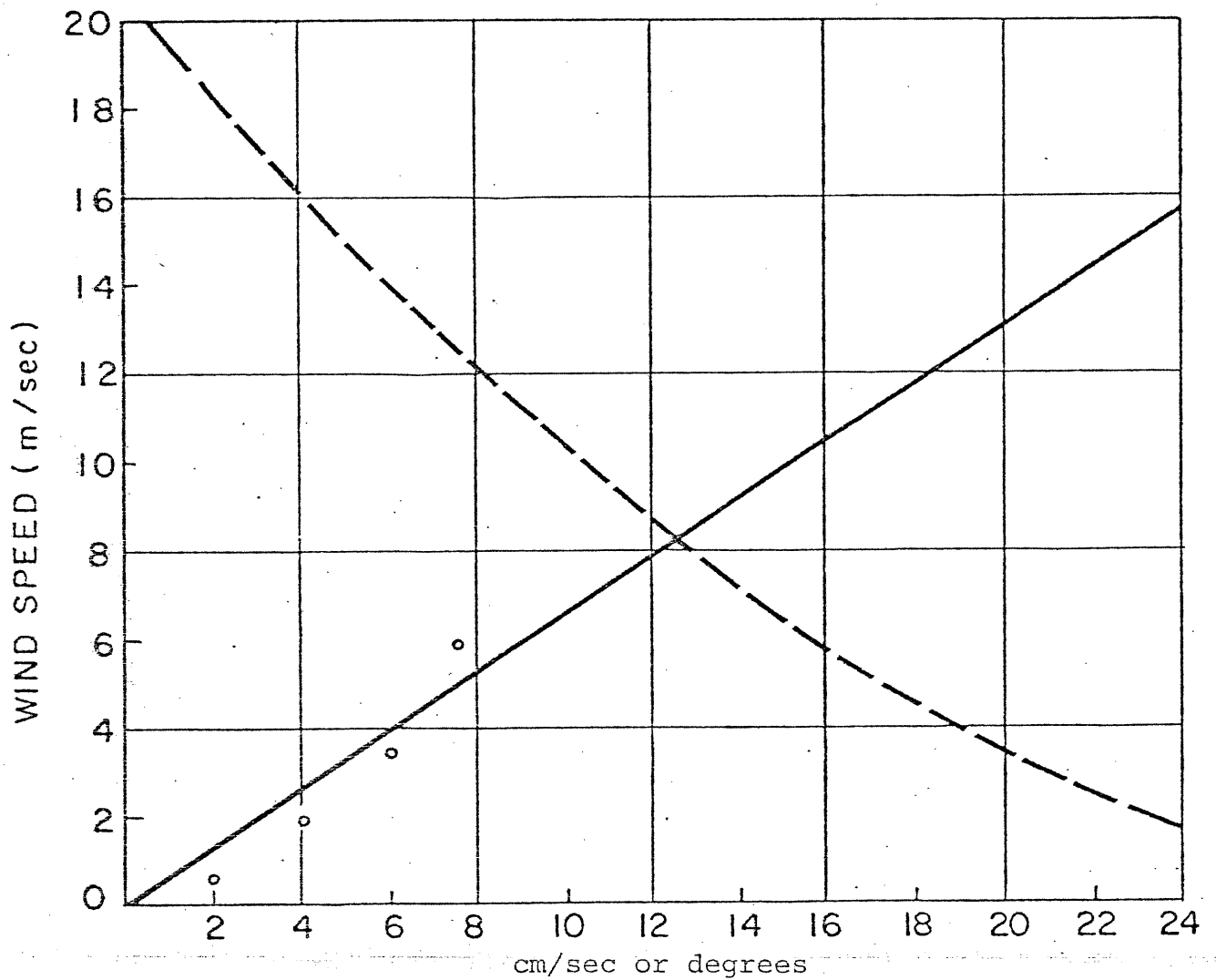Figure 35. Bottom currents for two hour ebb tide period H4-L0.

Figure 36. Current speed (cm/sec) solid line and current deflection (degrees right) dashed line, as a function of wind speed (m/sec). For latitude 43°38'N. From Thorade (1914).